ANNUAL REVIEWS

Annual Review of Astronomy and Astrophysics

Theoretical Challenges in Galaxy Formation

Thorsten Naab[1] and Jeremiah P. Ostriker[2,3]

[1]Max Planck Institute for Astrophysics, 85741 Garching, Germany; email: naab@mpa-garching.mpg.de

[2]Department of Astronomy, Columbia University, New York, NY 10027; email: jpo@astro.columbia.edu

[3]Department of Astrophysical Sciences, Princeton University, Princeton, NJ 08544

Annu. Rev. Astron. Astrophys. 2017. 55:59–109

First published as a Review in Advance on June 2, 2017

The *Annual Review of Astronomy and Astrophysics* is online at astro.annualreviews.org

https://doi.org/10.1146/annurev-astro-081913-040019

Keywords

theoretical models, cosmology, galaxy evolution

Abstract

Numerical simulations have become a major tool for understanding galaxy formation and evolution. Over the decades the field has made significant progress. It is now possible to simulate the formation of individual galaxies and galaxy populations from well-defined initial conditions with realistic abundances and global properties. An essential component of the calculation is to correctly estimate the inflow to and outflow from forming galaxies because observations indicating low formation efficiency and strong circumgalactic presence of gas are persuasive. Energetic "feedback" from massive stars and accreting supermassive black holes—generally unresolved in cosmological simulations—plays a major role in driving galactic outflows, which have been shown to regulate many aspects of galaxy evolution. A surprisingly large variety of plausible subresolution models succeeds in this exercise. They capture the essential characteristics of the problem, i.e., outflows regulating galactic gas flows, but their predictive power is limited. In this review, we focus on one major challenge for galaxy formation theory: to understand the underlying physical processes that regulate the structure of the interstellar medium, star formation, and the driving of galactic outflows. This requires accurate physical models and numerical simulations, which can precisely describe the multiphase structure of the interstellar medium on the currently unresolved few hundred parsec scales of large-scale cosmological simulations. Such models ultimately require the full accounting for the dominant cooling and heating processes, the radiation and winds from massive stars and accreting black holes, and an accurate treatment of supernova explosions as well as the nonthermal components of the interstellar medium like magnetic fields and cosmic rays.

Contents

1. INTRODUCTION

1.1. What Do We Want to Learn?

Do we understand galaxy formation? Galaxies have been called the building blocks of the Universe, and they are clearly the fundamental units within which stars are organized. They do show characteristic sizes ($R_{\rm gal} \sim$ kiloparsec) and masses ($M_{\rm gal} \sim 10^{10}\,{\rm M}_\odot$). Their abundance ($\sim 10^{-2}$ Mpc^{-3}) is set by their characteristic mass and the fact that they constitute a moderate fraction ($f_{\rm gal} \sim 10\%$) of the cosmic baryon budget. Can we derive these numbers ($R_{\rm gal}$, $M_{\rm gal}$, $f_{\rm gal}$) from first principles? Can we, from straightforward numerical simulations, chart the history of when, where, and how the formation and evolution of galaxies occurred? And, finally, do we understand it all well enough to characterize the internal properties of these systems, their ages, kinematics, and mass distributions, and their organization into families having properties describable using relatively few parameters?

As a problem in physics, there are four clearly definable aspects: (*a*) specification of the initial conditions; (*b*) knowledge of the physical processes primarily responsible for understanding each phase of galactic evolution; (*c*) computational tools that permit us to start with aspect a, utilize aspect b to construct models predicting the detailed properties of representative samples of galaxies; and (*d*) tests by direct comparison with the rich treasury of information provided by nature and revealed by modern observational technology.

We argue that the current, standard cosmological models are sufficiently accurate to provide initial conditions as required to any specified accuracy. With regard to physical processes, the problem is divided into two parts: (*A*) What would the evolution be if we only had to consider dark matter, and (*B*) how is the picture altered if we include the primordial radiation fields, the

baryonic gas as well as the energy, processed interstellar matter, and momentum input from the stars and massive black holes? The current state of the art shows a good grasp of problem A—different investigators using different codes recover quite similar descriptions of the Universe; but with regard to the more complex problem B—allowing for feedback from stars and black holes, we have only preliminary gropings toward physical understanding. One simple example suffices. The nonthermal and relativistic components of the ISM—magnetic fields and cosmic rays (CRs)—are not thought to be primordial but in our Galaxy have energy densities comparable with kinetic energy densities, which are significantly higher than thermal energy densities (e.g., Boulares & Cox 1990, Ferrière 2001). Are these components essential to understanding galaxy formation or are they mere byproducts? They are not included in most treatments, and the omission may (or may not) be crucial. However, the situation is improving.

As a result of our success with regard to problem A—the "stage setting" so to speak—we have a moderately good grasp of the physics that determines the approximate values of the three scales, the numbers for size, mass, and abundance, noted as the fundamental characteristics of galaxies, but we have a poor knowledge of the details that are important in determining the internal structure and evolution of these systems. Finally, our computational tools are marginally adequate for the simpler part (A) of the task, but they are perhaps not up to the challenge of the multidimensional, multicomponent, time-dependent computation involving the necessary range of temporal and spatial scales.

So far, we have been describing this as an ab initio problem of physics, like the motion of a playground swing—though more complex—but, of course, this is not the way that the history unfolded. Observational discoveries have guided us every step of the way, often pointing out to us how oversimplified our models have been. These observations have been of two kinds, those that describe the Universe as it is (e.g., galaxy rotation curves or the details of the multiphase ISM) and those that tell us of the time development, either through using the archaeological method of examining the stellar populations of nearby galaxies and determining when/how the various components were assembled, or by using the Universe as a time machine and looking at the progenitor populations at earlier cosmic epochs. In any case, direct observations are the facts that all models have to be tested against, and in most cases they are the drivers for progress in theoretical galaxy formation, both on the small scales of individual galaxies as well as on the large-scale distribution and redshift evolution of galaxy populations.

Galaxy formation has become such a large field in astrophysics that a full overview of all theoretical challenges is beyond the scope of a single review. Here, we focus on a subset of problems in computational astrophysics. Numerical implementations of "feedback" processes have traditionally been tested with idealized galaxy models and merger simulations. These models have resulted in important insights on star formation, morphological and kinematic transformations, merger-driven gas flows, triggering of star formation, the impact of accreting black holes on the termination of star formation, and size evolution. We give an overview of these feedback models and their use in modern cosmological simulations of galaxy formation. We briefly highlight major steps forward like the successful simulation of spiral galaxies and the cosmological evolution of galaxy populations. Some other major theoretical challenges that can be addressed with cosmological galaxy formation simulations are not discussed here in detail. One of these is how galaxies accrete their gas. Gas accretion is a necessary and fundamental process for galaxy formation, but surprisingly it has not yet been conclusively observed. From numerical studies it is still unclear whether the gas accreted onto the galaxies is from cold filaments (Kereš et al. 2005, Dekel et al. 2009) or whether the filaments dissolve in the halos and accretion is more smooth (Nelson et al. 2013). A related question is how galactic outflows actually transport metal-enriched material into the circumgalactic medium (see, e.g., Oppenheimer & Davé 2006, Schaye et al. 2015). This is also

a numerically challenging question, as the spatial resolution in the halos of galaxies is typically much lower than in the dense regions, and mixing processes are highly complex (e.g., Scannapieco & Brüggen 2015). We also do not address issues that test galaxy formation on small scales in the context of the underlying cold dark matter cosmological model like the "too big to fail" problem (Boylan-Kolchin et al. 2011) or the question of whether small dark matter halos have cusps or cores (e.g., Kravtsov et al. 1998, Pontzen & Governato 2012). We accept the standard cold dark matter paradigm because of its numerous proven successes on large scales while fully aware of the challenges it faces on small scales. Instead, we focus on the physics of the ISM. The ISM strongly influences galaxy formation. Many processes determining star formation and galactic outflows as well major observable features act in the ISM, and a better understanding and more accurate modeling of theses processes are, in our view, the major theoretical challenge for galaxy formation in the future.

1.2. Some Relevant Observations

Our summary of observations that put important constraints on theoretical galaxy formation models will necessarily be brief and does not attempt to provide a full list of references. The first and most obvious is the observational information accumulated in the past century specifying the four principle components of all massive galaxies: stars, gas, dark matter, and supermassive black holes.

1.2.1. Stars. From Hubble's time onward, we realized that the bulk of the mass in the visible parts of galaxies resides in one of two components, a spheroidal part having a scale length typically of only a few kiloparsecs to a few tens of kiloparsecs with a roughly de Vaucouleurs surface density profile (de Vaucouleurs 1948) and a flattened, rotationally supported disk/spiral component, which is typically somewhat larger (apart from the highest mass systems) and has a roughly exponential profile (e.g., Shen et al. 2003, Blanton & Moustakas 2009, van der Kruit & Freeman 2011). These two components appear to be distinct, and environmental considerations must be important in understanding their formation, because isolated systems tend to be disk dominated and those in regions of high galactic density tend to be dominated by the spheroidal component (e.g., Dressler 1980, Blanton & Moustakas 2009, Kormendy et al. 2010, Cappellari et al. 2011a). Recent integral field studies have significantly improved our understanding of the complex kinematics of galaxies (de Zeeuw et al. 2002, Cappellari et al. 2011b, Sánchez et al. 2012, Fogarty et al. 2014, Bundy et al. 2015). Stellar dating indicates extended and relatively flat star-formation histories for the disks with typical ages of a few billion years and peaked star-formation histories with typical stellar ages of ∼10 billion years for massive early-type galaxies (e.g., Kauffmann et al. 2003, Heavens et al. 2004, Thomas et al. 2005, Renzini 2006, Kormendy et al. 2009). Large surveys made it possible to observe relatively accurate stellar mass functions not only in the local Universe (e.g., Pérez-González et al. 2008, Li & White 2009, Bernardi et al. 2013) but also toward higher redshifts (e.g., Bouwens et al. 2012, Moustakas et al. 2013, Muzzin et al. 2013, Duncan et al. 2014, Song et al. 2016).

1.2.2. Gas. Typical Milky Way–like spiral galaxies have roughly ∼10% of their mass in cold ISM gas ($\lesssim 10^4$ K). An even larger fraction (some of it hotter and ionized) of gas might be stored in the so-called circumgalactic medium, the region extending from the star-forming ISM into the galaxy halos (e.g., Werk et al. 2014, Somerville & Davé 2015). More massive early-type galaxies typically have significantly lower cold gas fractions, although they are not devoid of cold gas, contrary to the traditional picture (Catinella et al. 2010, Saintonge et al. 2011, Young et al. 2011, Serra

et al. 2012). Massive early-type systems are usually embedded in hot ($>10^5$ K) X-ray–emitting gas comprising a significant fraction of the total baryonic mass (e.g., Mulchaey 2000, Vikhlinin et al. 2006, Giodini et al. 2009, Sun et al. 2009, Dai et al. 2010, Kravtsov & Borgani 2012, Renzini & Andreon 2014, Anderson et al. 2015).

1.2.3. Dark matter. Following Zwicky's and Babcock's work in the 1930s and then the work of many authors on the rotation curves of normal galaxies in the 1970s and 1980s (e.g., Sofue & Rubin 2001), it became apparent that the stars in most normal galaxies are embedded in massive halos composed of some unknown type of dark matter with a total mass and size roughly 10 times that of the stellar component. The generally flat observed rotation curves of spiral galaxies are an important test for cosmological formation models (see Courteau et al. 2014). Recent results from strong lensing have contributed to our knowledge of the dark matter content of massive galaxies, which have typical contributions of 5–20% within their stellar half-light radii (e.g., Koopmans et al. 2009, Treu 2010; see also lensing measurements of the stellar-to-halo mass ratio, Mandelbaum et al. 2006). Dwarf galaxies like Sculptor or Fornax or the recently discovered category of large ultradiffuse galaxies (c.f. van Dokkum et al. 2015) are dominated by dark matter throughout (see also Kormendy & Freeman 2016).

1.2.4. Supermassive black holes. A number of studies have indicated that supermassive black holes typically reside in the centers of normal galaxies (having stellar masses $\gtrsim 10^{10.3}$ $M_\odot$), with their masses tightly correlated with the masses (and stellar velocity dispersions) of the spheroidal components of the galaxies, the ratio being roughly 5:1,000 [see, e.g., Genzel et al. (1997) and Kormendy & Ho (2013) for reviews]. Given the evident association with active galactic nuclei (AGNs), it is widely believed that the energy emitted by these monsters during their formation is roughly 10% of their rest mass (Shakura & Sunyaev 1973, Soltan 1982), which makes them competitive with high-mass stars with regard to energy input (in various forms) into the surrounding galaxies (e.g., Silk & Rees 1998).

1.2.5. The Milky Way. The archaeological method was used very successfully in the last half of the twentieth century to reconstruct a plausible history of our own Galaxy, the Milky Way. The Sun is a typical star in the disk component that gradually formed from relatively metal-rich gas. It appears that this disk component grew slowly, in size and mass, as rotationally supported gas was steadily turned into stars over cosmic time, and the typical stars in our cosmic neighborhood were formed only 3–6 billion years ago, which is relatively late in the evolution of the Universe. The fact that much less than 10% of the disk stellar mass has a metallicity that is less than 10% of the latest formed stars tells one immediately that the disk is temporally a secondary structure heavily contaminated by the metal-rich ejecta from earlier stellar generations (Ostriker & Thuan 1975). The age distribution tells us that it formed "inside-out" with the stars in the low-metallicity, gas-rich outer parts of the disk formed most recently (see, e.g., Rix & Bovy 2013). The somewhat triaxial, bar-like, inner structure is old and may have formed via the instability of a cold rotating disk (e.g., Ostriker & Peebles 1973), but the outer spheroidal halo is likely the debris from infalling, captured, smaller systems that has accumulated over time. The stars in this extended spheroidal (or elliptical) component are typically ~10 billion years old, are lower in heavy-element abundances, and tend to have an isotropic or even somewhat radially biased distribution of orbits.

Most of the stars (the fraction might be as high as $\gtrsim$95%) in our Galaxy were made from gas that was added to the Galaxy, forming into stars within the system, and only a very small fraction of the stellar mass comes from stars made in other galaxies that were added to our system via galactic

mergers (Kennicutt & Evans 2012). Thus major mergers might not have been at all important in the late formation history of our Galaxy or of others with very similar structures.

Work by Eggen et al. (1962) in the early 1960s provided solid evidence that our Galaxy began in phase of dramatic collapse. Other spheroidal systems observed in detail, though more massive and more metal rich, seemed to be composed of stars of similar age and orbital properties, so it was plausible that they formed by a similar process. In this simple picture the disk is a later addition as higher angular momentum, already contaminated material drifted into the galaxy, accumulated in a rotating disk, and was gradually turned into the bulk of the stars. This provides a natural explanation for the two components of the Hubble classification and also a reason for the absence of the disk components in dense environments within which tidal or ram-pressure effects prevent the late formation of disks. Although the details of this story have evolved, the overall picture has withstood the test of time remarkably well. The archaeological approach to galaxy formation and evolution continues, with much useful work being done in teasing out the details of how the extended spheroidal component was put into place. If this picture is correct, then in the much more massive elliptical galaxies like M87 the secondary, stellar component added by the cannibalization of numerous smaller systems may comprise 20% and up to 50% of the total, in contrast to the much smaller fraction of accreted stars in the common, lower-mass, disk-like spiral systems.

The Milky Way also holds the most information about the detailed structure of the multiphase ISM. Most of the gas is found in three phases: the cold neutral medium, the warm neutral medium, and the hot ionized medium. The hot phase fills about 30% of the volume (Ferrière 2001) in the disk but dominates no further than a few kiloparsecs from the disk midplane (see Kalberla & Kerp 2009, and Section 3).

1.3. Learning from Galaxy Evolution with Redshift

Observations of galaxies extending toward higher redshift (and thus earlier times) have given additional insight into galaxy properties of fundamental importance. In the following we refer to some of the relevant observational work.

1.3.1. Ubiquitous winds. Galactic winds, with velocities up to 500 km s^{-1} and most likely of biconical nature, carrying large amounts of material out of star-forming galaxies (the rate being comparable with and higher than the star-formation rate) are ubiquitous not only in the nearby Universe (e.g., Heckman et al. 1990, 2000; Martin 1999; Veilleux et al. 2005; Rubin et al. 2014) but also at higher redshift at the cosmic peak of conversion of gas into stars (Pettini et al. 2001, Steidel et al. 2010, Shapley 2011, Martin et al. 2013). At low as well as high redshift these winds most likely enrich the circumgalactic medium with gas, metals, and possibly magnetic fields (Steidel et al. 2010, Bernet et al. 2013, Werk et al. 2014), providing the material that, if falling back in at later times with added angular momentum (Peebles 1969), can be the source of the secondary disk systems. These winds transport gas out of the galaxies at rates similar to those at which gas is converted into stars and therefore have to be of importance for regulating the formation efficiency of stars in galaxies. Even at high redshift the launching sites of star-formation-driven (S.F. Newman et al. 2012) and AGN-driven (Genzel et al. 2014) winds can now be resolved with modern instruments.

1.3.2. Size evolution of early-type galaxies. Today's massive ($\sim 10^{11}$ $M_\odot$) early-type galaxies could have formed early and become "red and dead" by $z \sim 2$, being much smaller systems ($\sim$1 kpc) than those seen today. Their growth in size (while not forming stars) could be understood as a likely sign of subsequent addition of stars in minor mergers at larger radii (e.g., Daddi et al. 2005, Trujillo et al. 2007, van Dokkum et al. 2010, Damjanov et al. 2011). Observations of significant

structural evolution of massive early-type galaxies disfavor any singular monolithic collapse or binary merger formation scenario (van Dokkum et al. 2008). Also the observed strong increase in size and the weak decrease in velocity dispersion (Cenarro & Trujillo 2009) of the early-type galaxy population as a whole, which also includes additions to the red sequence at lower redshifts (see, e.g., Patel et al. 2013b, van der Wel et al. 2014, Fagioli et al. 2016), poses tight constraints on any formation model. From the observed age distribution of stars in normal massive early-type galaxies, we know that the substantial observed evolution was not caused primarily by the addition of newly formed stars but rather the addition and rearrangement of old stars in these systems.

1.3.3. Evolution of spiral galaxies. The high-redshift progenitors of Milky Way–like disk systems are also smaller than local examples of similar systems and have formed half of their mass below $z \sim 1$. Most of the mass is assembling at larger radii by in situ star formation, providing direct evidence for inside-out growth accompanied by mass growth in the central regions that can be dominated by bars and bulges (Patel et al. 2013a). The central mass growth might originate from secular instabilities or merger events, but most stars currently in spiral systems were made from gas added to them rather than from accreted stars or stellar systems. In general the size evolution of spiral systems is, however, significantly less rapid than it is for early-type galaxies (van der Wel et al. 2014).

1.3.4. Evolution of star-formation rates and gas fractions. A significant fraction (if not most) of the stars in the Universe have been formed in galaxies with star-formation rates that are almost linearly related to their stellar mass (the star-formation main sequence) since $z \sim 2.5$ (see, e.g., Daddi et al. 2007, Noeske et al. 2007, Whitaker et al. 2012, Renzini & Peng 2015). The tightness of the overall relation and the mostly disk-like morphology (Genzel et al. 2006, Förster Schreiber et al. 2009) of the highly star-forming systems indicate that major merger–driven starbursts are of minor importance for the universal star-formation budget. The increase in star-formation rate (the normalization of the main sequence) toward high redshift is accompanied by increasing gas fractions reaching up to ∼50% at redshift $z \sim 2$ (e.g., Daddi et al. 2010; Tacconi et al. 2010, 2013). This buttresses the simple picture that most star formation comes from the gradual transformation of accumulated gas into stars.

1.4. Methods of Solution

Let us return now to the physics problem to be solved given this observational background. First, we look at what we have described as problem A, the evolution of radiation fields, dark matter, and gas in the standard cosmological paradigm. This has been well summarized in several recent textbooks (e.g., Mo et al. 2010), so only some of the highlights need to be mentioned. A spectrum of adiabatic perturbations is imprinted onto the three components at high redshift, producing cosmic microwave background radiation fluctuations emitted at roughly redshift 1,000, the analysis of which (cf. WMAP, *Planck*) uniquely specifies the cosmological model (Spergel et al. 2007, Planck Collaboration et al. 2014). If we take that to be the simplest one compatible with the data (the ΛCDM cosmologically flat model), the model can be defined by five to six independent parameters that are typically known now (primarily, but not entirely, from analysis of the cosmic microwave background radiation) to high accuracy. The composition of the dark matter remains unknown, but the standard cold dark matter model has been so successful that the principal remaining alternatives, warm dark matter or fuzzy dark matter, behave essentially like ΛCDM on all large scales with (interesting) deviations becoming apparent below ∼1 kpc.

1.4.1. Direct simulations of dark matter. Accepting this model, we can specify in a cosmologically representative volume the statistical distribution of gas, dark matter, and radiation in a fashion sufficiently detailed to provide initial conditions for computation of the evolution of the various components. In the simplest treatments of this evolution, dark matter is followed via Newton's laws, and the transformation of gas into stars and black holes is ignored. Many different groups have worked on the problem, producing extraordinarily successful (and convergent) results (see Frenk & White 2012). The Millennium simulation (Springel et al. 2005c) was perhaps the most publicly successful dark matter calculation, but other simulations (Klypin et al. 2011) also of larger volumes (Angulo et al. 2012) or constrained to a certain halo mass scale (Diemand et al. 2007, Springel et al. 2008, Stadel et al. 2009, Gao et al. 2012) have made very important contributions. This is problem A, and it is essentially a solved problem. But it leaves us a long way from understanding the evolution of real galaxies composed primarily of stars.

1.4.2. Semianalytical models for baryons. There exist different approaches to the more difficult problem B, that of the allowance for star and black hole formation, and the input from these sources of mass, energy, momentum, and processed matter back into the gaseous component. The first approach to this hard problem was to set up comprehensible "model problems," the solutions of which would be illuminating. One large class of such efforts has been broadly labeled the semianalytic method, where one takes the dark matter simulations as a given and then tries, by one means or another, to estimate how the other components will react. Examples of progress made in the late 1990s via the setting and solving of very informative model problems consider the formation of disks from gas accumulating within dark matter halos (Dalcanton et al. 1997, Mo et al. 1998). Modern attempts to input what are thought to be the most important physical processes in a simple fashion (e.g., Kauffmann et al. 1993, Somerville & Primack 1999, Bower et al. 2006, Croton et al. 2006, Guo et al. 2011, Henriques et al. 2015) aim to find the set of processes that best produce realistic mock observations (see the review by Somerville & Davé 2015). Another class of more analytical models makes the simplifying assumption that star-forming galaxies evolve in a quasi-equilibrium fashion regulated by gas inflow and outflow, star formation, and the change of mass in the galactic gas reservoir. The above approaches are extensively reviewed by Somerville & Davé (2015).

1.4.3. Direct simulations including baryons. Although these methods have been most helpful in furthering our understanding, the technical and algorithmic progress has enabled the direct and ambitious effort to include as much of the detailed physics as possible and simply compute forward from the well-established initial conditions to the current time using gravity, hydrodynamics, radiation transfer, and all of the elaborate apparatus developed by physics to address continuum mechanics. The computational tools to follow the evolution of dark matter and stars (gravity) as well as gas (hydrodynamics) have been developed since the early 1980s.

The first three-dimensional coupled hydrodynamical simulations including self-gravity used the smoothed particle hydrodynamics (SPH) technique (Efstathiou & Eastwood 1981, Evrard 1988, Hernquist & Katz 1989). The Lagrangian particle based SPH method [Gingold & Monaghan 1977, Lucy 1977; see also Springel 2010a and Somerville & Davé 2015 for recent reviews] is relatively simple to implement and, due to its adaptive spatial resolution and good conservation properties, has been very popular for galaxy-formation simulations until today. However, the basic implementation has to be modified for typical astrophysical conditions including shocks, shear, and large temperature gradients, and it has become clear that some standard implementations have serious difficulties in properly modeling fluid mixing and subsonic turbulence (Agertz et al. 2007, Springel 2010a). Most of the recent SPH work on cosmological galaxy formation is

based on derivatives of either the GASOLINE (Wadsley et al. 2004) code or the GADGET (Springel 2005) code and includes updated implementations to treat the mixing problem better (see, e.g., Wadsley et al. 2008, Read & Hayfield 2012, Hopkins et al. 2014, Hu et al. 2014, Schaller et al. 2015, Schaye et al. 2015, and references therein). As an alternative to the SPH method, particle-based meshless-finite-mass and meshless-finite-volume methods have been proposed (Gaburov & Nitadori 2011). The recent GIZMO implementation is based on the GADGET framework and shows some significant improvements on idealized test problems, in particular for low Mach number gas (Hopkins 2015).

Eulerian hydrodynamic codes have also been widely used for cosmological simulations, some with adaptive mesh refinement (AMR) capabilities. These codes typically perform better than SPH in terms of mixing and shock problems but might suffer from artifacts owing to grid structure and numerical diffusion, which, for some solvers, can become significant. The first rough Eulerian treatment was conducted by Cen & Ostriker (1992a), and the recently most used, greatly improved, Eulerian AMR codes are ENZO (Bryan et al. 2014), RAMSES (Teyssier 2002), and ART (Kravtsov et al. 1997), and also FLASH (Fryxell et al. 2000) as well as ATHENA (Stone et al. 2008) for ISM simulations on smaller scales. The newly developed moving-mesh code AREPO (Springel 2010b) similarly suffers from numerical diffusion but combines advantages of the Lagrangian and Eulerian approaches and performs much better than traditional SPH codes like GADGET on mixing problems with a high convergence rate (Springel 2010a, Sijacki et al. 2012).

There are ongoing efforts to better understand the strengths and weaknesses of different numerical schemes (e.g., Price & Federrath 2010, Heitsch et al. 2011, Hubber et al. 2013, Hayward et al. 2014, Kim et al. 2014) and to constantly improve on accuracy and performance of all major codes. It was realized early on that different numerical schemes applied to cosmological simulations can result in systems with different physical properties (Frenk et al. 1999), even if only gravity and hydrodynamics are considered. In addition, there is a wealth of published subresolution models (see Section 2.2.1) that are used to model galaxy formation. These models are often designed for particular numerical schemes and introduce even stronger variations in physical properties for a given set of initial conditions (Scannapieco et al. 2012). One of the major challenges in computational galaxy formation is to further improve on the numerical schemes and reduce the contribution of subresolution modeling to numerically resolved physical scenarios.

These numerical methods, which we could label ab initio computations aiming to solve problem B, are discussed in the second part of this review. But first, we address two other extremely useful idealized and empirical approaches that preceded and accompanied them.

1.5. Disks, Ellipticals, and Mergers: A Very Useful Set of Idealized Simulations

In the early 1970s a definite cosmological model had not emerged, and the computational resources as well as the numerical algorithms were still limited. This was the start of idealized merger simulations, as it had been realized that galaxies actually interact and merge for bridges, tidal tails, and other merger phenomena that had been observed (Toomre & Toomre 1972, Joseph & Wright 1985, Sanders et al. 1988). Early self-consistent *N*-body simulations (e.g., White 1978) were limited to the stellar component of galaxies with a few hundred gravitating particles (stars), a situation that has significantly improved until now when millions of star particles, dark matter particles, and complicated gas dynamical processes can be studied (e.g., Hopkins et al. 2013a). With methods for creating equilibrium models for multicomponent galaxies (i.e., Hernquist 1993b) it became possible to simulate the evolution of the stellar and gaseous components of disk galaxies in more detail. For more than 20 years such setups have been playing a major role for developing star formation and feedback models in direct comparison with observations of star-forming spiral

galaxies (e.g., Mihos & Hernquist 1994a, Springel & Hernquist 2003, Li et al. 2005, Dalla Vecchia & Schaye 2008, Hopkins et al. 2011, Agertz et al. 2013). In most cases tests are conducted to determine under which conditions a given model reproduces the observed relation between gas surface density and star-formation rate surface density (Kennicutt 1998). Only successful models are then considered for more complex simulations of galaxy mergers or the cosmological formation of galaxies.

A number of important physical processes have been investigated with merger simulations, and the insight into galaxy formation physics has been significant. We know that equal-mass mergers are rare and relatively unimportant for the cosmic star-formation budget (see Section 1.3.4 and Bluck et al. 2009, Williams et al. 2011, Man et al. 2012). For intermediate-mass galaxies (e.g., the Milky Way) and low-mass systems, stars are primarily formed from streams of gas that accumulate centrally or in disks (e.g., Rodriguez-Gomez et al. 2016, Qu et al. 2017). For high-mass systems (i.e., massive early-type galaxies) mergers become important. Stars added in major and minor mergers can make up as much as 50% of the largely outer envelopes (in the case of minor mergers) of these systems (Naab et al. 2009, Rodriguez-Gomez et al. 2016, Qu et al. 2017). But the initial proposal that normal ellipticals are made by morphological transformations of disk galaxies in binary major mergers of spirals, though not generally applicable (Ostriker 1980), is influential and instructive. In particular, observed nearby disk galaxy mergers were shown to be most likely to evolve into systems with structural similarities to young early-type galaxies (e.g., Rothberg & Joseph 2004).

1.5.1. Collisionless mergers. There are two groups into which merger simulations might be separated. Collisionless simulations of stars and dark matter mutually interacting by gravity alone were evolved by the collisionless Boltzmann equation (see, e.g., Binney & Tremaine 2008). Such idealized systems can be considered energy conserving (no radiative losses). In reality almost no galactic system meets these conditions. Even massive galaxies have some amount of hot and cold gas (e.g., Sun et al. 2009, Young et al. 2011, Serra et al. 2012). But if the gas components can be considered dynamically unimportant it is justified to consider a system collisionless (the term dry has been used in the literature). When spheroidal one-component systems merge, their structural evolution can—to good accuracy—be estimated using the virial theorem with only a few assumptions (Cole et al. 2000, Bezanson et al. 2009, Naab et al. 2009). Following Naab et al. (2009) one can assume that a compact initial stellar system has formed (e.g., involving gas dissipation) with a total energy E_i, a mass M_i, a gravitational radius $r_{g,i}$, and the mean square speed of the stars is $\langle v_i^2 \rangle$. According to the virial theorem (Binney & Tremaine 2008) the total energy of the system is

$$\begin{aligned} E_i &= K_i + W_i = -K_i = \frac{1}{2} W_i \\ &= -\frac{1}{2} M_i \langle v_i^2 \rangle = -\frac{1}{2} \frac{G M_i^2}{r_{g,i}}. \end{aligned} \quad (1)$$

This system then merges (on zero energy orbits) with other systems of a total energy E_a, total mass M_a, gravitational radii r_a, and mean square speeds averaging $\langle v_a^2 \rangle$. The fractional mass increase from all the merged galaxies is $\eta = M_a/M_i$, and the total kinetic energy of the material is $K_a = (1/2) M_a \langle v_a^2 \rangle$, further defining $\epsilon = \langle v_a^2 \rangle / \langle v_i^2 \rangle$. Here $\epsilon = 1$ represents an equal mass merger, and $\epsilon \sim 0$ represents very minor mergers. Under the assumption of energy conservation Khochfar & Burkert (2006) indicate that most dark matter halos merge on parabolic orbits; the ratio of initial to final mean square speeds, gravitational radii, and densities can be expressed as

$$\frac{\langle v_f^2 \rangle}{\langle v_i^2 \rangle} = \frac{(1+\eta\epsilon)}{1+\eta}, \frac{r_{g,f}}{r_{g,i}} = \frac{(1+\eta)^2}{(1+\eta\epsilon)}, \frac{\rho_f}{\rho_i} = \frac{(1+\eta\epsilon)^3}{(1+\eta)^5}.$$

For binary mergers of identical systems, $\eta = 1$, the mean square speed remains unchanged, the size increases by a factor of 2, and the densities decrease by a factor of 4. In the limit that the mass is accreted in the form of a weakly bound stellar system with $\langle v_a^2 \rangle \ll \langle v_i^2 \rangle$ or $\epsilon \ll 1$, the mean square speed is reduced by a factor of 2, the size increases by a factor of 4, and the density drops by a factor of 32. These estimates are, however, idealized assuming one-component systems, no violent relaxation, and zero-energy orbits with fixed angular momentum. In the presence of a dark matter halo the structural changes become more complicated and, e.g., the fraction of dark matter at the center (inside the half-mass radius of the stars) may increase because of violent relaxation (Boylan-Kolchin et al. 2005, Hilz et al. 2012). In general a fraction of the orbital angular momentum of the galaxies is transferred to rotation in the central galaxy, so that the merger remnants in most cases rotate significantly (White 1979a, Naab et al. 2006b, Di Matteo et al. 2009a, Bois et al. 2010, Bois 2011). Major mergers of spheroidal galaxies are also expected to flatten existing abundance gradients (White 1979b, Di Matteo et al. 2009b).

If a spheroidal system experiences collisionless minor mergers (with satellite galaxies of much lower mass than the central), violent relaxation effects in the central galaxy are negligible and the satellite stars are stripped at larger radii (Villumsen 1983), a mechanism that offers a plausible explanation for the observed structural evolution of massive galaxies (Nipoti et al. 2003, Hilz et al. 2012) and the formation of extended stellar envelopes in early-type galaxies leading to the very high observed Sérsic indices and outer metallicity gradients (Villumsen 1983, Hilz et al. 2013). Whether minor mergers alone can explain the observed strong size evolution of massive early-type galaxies will depend on the actual merger rates as well as the structure of the satellite galaxies (Nipoti et al. 2009, Cimatti et al. 2012, A.B. Newman et al. 2012 , Bédorf & Portegies Zwart 2013, Oogi & Habe 2013). Per added unit of stellar mass this process can also increase the fraction of dark matter within a half-mass radius more efficiently than major mergers (Boylan-Kolchin et al. 2005, Hilz et al. 2013).

Another important process investigated is the morphological transformation of kinematically cold disk galaxies to kinematically hot spheroidal galaxies (Farouki & Shapiro 1982, Negroponte & White 1983, Barnes 1992, Barnes & Hernquist 1992, Hernquist 1992). Violent relaxation heats the disk stars; then some fraction of the orbital angular momentum and the spin of the initial disk systems can be absorbed by the dark matter halos (Barnes 1988). This results in stellar remnants that can have early-type galaxy morphology and kinematics if the progenitor galaxies had a bulge component of sufficiently high phase space density (Hernquist 1993a). Therefore merging is important for the formation of hot stellar systems. Depending on the mass-ratio of the merging disks—and the amount of damage that is done to the primary disk, the remnants rotate fast or slow; have disky, round, or boxy isophotal shapes; and are more or less flattened (Heyl et al. 1994; Barnes 1998; Bekki 1998; Naab et al. 1999; Bendo & Barnes 2000; Cretton et al. 2001; Naab & Burkert 2003; Bournaud et al. 2004, 2005; González-García & Balcells 2005; Jesseit et al. 2009). For very low-mass infalling systems the disk might be only moderately heated and retains its flat and rotationally supported morphology for single events (Quinn et al. 1993, Velazquez & White 1999). Repeated minor mergers will make the initial disk system more spherical and reduce its spin (Bournaud et al. 2007, Qu et al. 2010).

1.5.2. Mergers with gas. A major step in understanding galaxy mergers was established once the simulations included a dissipative gas component. The gravitational torques exerted on the gas during the merger were able to drive the gas from large radii to the nuclear regions of the merger remnant once it lost its rotational support in tidally induced shocks (Barnes & Hernquist 1996). This has important implications for galaxy formation. Using subresolution models for the conversion of gas into stars (see Section 2.1), many studies showed that the gas inflow can trigger

a nuclear starburst similar to what is observed in ultraluminous infrared galaxies or ULIRGS, explaining observations of extra light in the centers of low-mass early-type galaxies (Mihos & Hernquist 1994c,b, 1996; Kormendy 1999; Springel 2000; Hopkins et al. 2009a,c, 2013a; Kormendy et al. 2009; Teyssier et al. 2010; Hayward et al. 2014). Gas accumulating at the center of merger remnants also makes the potential more spherical, favoring the population of stars on tube orbits (Barnes & Hernquist 1996, Jesseit et al. 2007). As a result, rotating remnants of gas-rich mergers can form disk-like subsystems (Bekki & Shioya 1997; Bendo & Barnes 2000; Barnes 2002; Jesseit et al. 2007, 2009) and show observed line-of-sight velocity distributions with steep leading wings, which is not the case if gas is neglected (Naab et al. 2006a; Hoffman et al. 2009, 2010).

The effect of dissipation in binary galaxy mergers has also been used to explain the detailed shape of scaling relations and the fundamental plane and its potential evolution with redshift (Cox et al. 2006a,b; Dekel & Cox 2006; Robertson et al. 2006b; Hopkins et al. 2009b). One branch of binary merger simulations was focused on the potential feeding of supermassive black holes, which are observed in most nearby early-type galaxies. Here the merger-triggered inflow provides the low angular momentum gas to be accreted onto the black hole (Hernquist 1989). However, the energy released from the accreting black hole has been suggested to drive gas out of the merger remnant, significantly reducing its star-formation rate (Springel et al. 2005a). The idea of black hole feedback to quench massive galaxies was born. Assuming a Bondi-like accretion and a relatively simple scaling for energy feedback in a subresolution model, it was also possible to provide an explanation for the observed stellar mass–black hole mass relation (Di Matteo et al. 2005). This finding has led to a number of studies based on idealized binary merger simulations investigating the evolution of the $M_{\rm bulge}$–$M_{\rm BH}$ and $\sigma_{\rm bulge}$–$M_{\rm BH}$ relation (e.g., Robertson et al. 2006c; Johansson et al. 2009a; Debuhr et al. 2010, 2011; Barai et al. 2014; Choi et al. 2014) and the evolution of the quasar luminosity function based on the assumption that most of the AGN activity is driven by galaxy mergers (e.g., Hopkins et al. 2005, 2006).

Despite the explanatory successes of these studies, the drawback of the idealized subresolution models used is that the actual physical processes (e.g., the feedback from central supermassive black holes) cannot be resolved, and the cosmological context is omitted. This is true for most merger simulations even though the typical spatial and mass resolution is much higher than in larger-scale cosmological simulations (Section 2). The assumptions are mostly simple, and physical effects are condensed or hidden in parameters or scale factors, which are often scaled to a specific set of observations (see Section 1.1). Therefore the validity of the astrophysical implications always remains somewhat uncertain. For example, many models adopted in binary merger simulations use a simple accretion scheme to determine the mass-flow rates onto the black holes. The accretion rate depends on the sound-speed of the surrounding medium, which can vary significantly depending on the assumed star formation and feedback model (see Section 2.3). Alternative models link the accretion rates to gravitational instabilities and torques (Hopkins & Quataert 2011, Hopkins et al. 2012a). Some models used for binary merger simulations assume feedback in the form of thermal energy to the gas surrounding the black hole (Springel et al. 2005a), whereas others take into account the observed momentum output that significantly reduces the amount of hot coronal gas and the observable X-ray luminosities (Debuhr et al. 2011, Choi et al. 2014). Binary merger experiments have been used as test beds for subresolution models used in larger-scale cosmological simulations.

1.5.3. Caveats of the merger hypothesis. The importance of major mergers for the formation and evolution of massive galaxies is still under debate. Idealized merger simulations ignore the cosmological context in which gas accretion and repeated minor mergers, as well as environmental

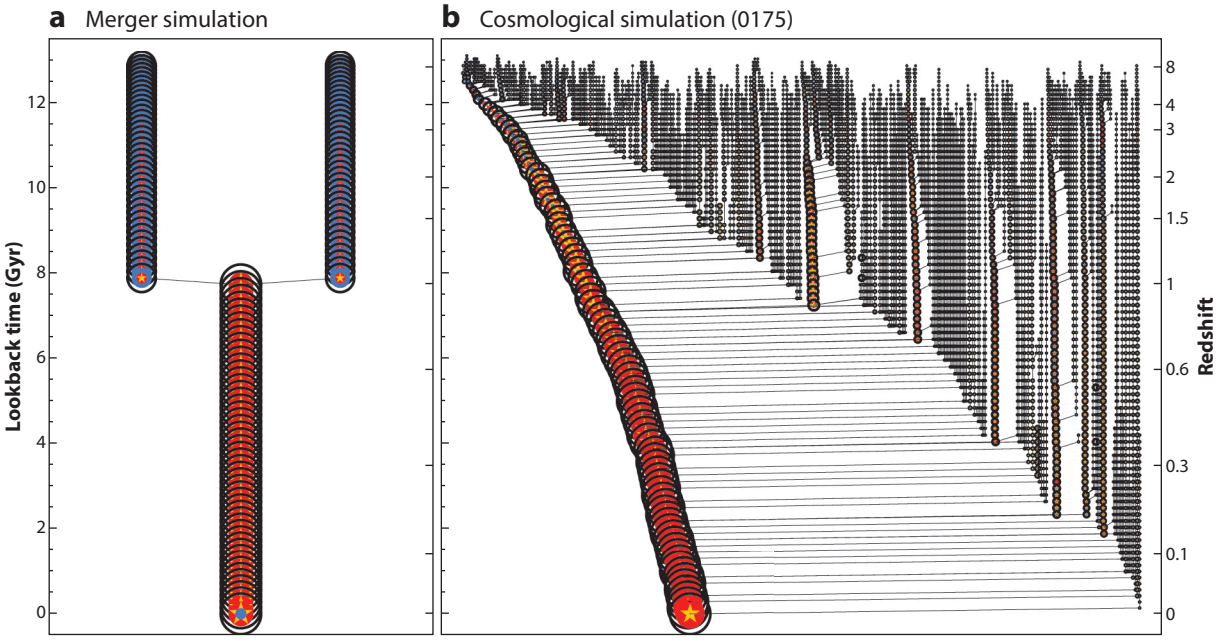

Figure 1

Binary disk merger simulations are useful in understanding merging disk galaxies observed in the sky. In general, they lack the realism and complexity of the cosmological assembly of old massive early-type galaxies. (*a*) A diagram and very simplified binary disk merger-tree. Two gas-rich (*blue*) stellar (*yellow*) disks with little hot gas (*red*) merge at $z \approx 1$ and form an elliptical galaxy. (*b*) A cosmological zoom shows a simulation of the formation of a dark matter halo (*black circles*), and its massive galaxy (cold gas: *blue*) is significantly more complex. It is evident that continuous infall of matter in small and large units is an important characteristic of the assembly of massive galaxies. The galaxy shown (0175 from Oser et al. 2010) is another extreme case as it has no major merger since $z \approx 3$. Other galaxies of similar mass can have up to three major mergers. Major mergers definitely happen, and they have a strong impact on galaxy evolution. Cosmological assembly and mass growth, however, is always accompanied by numerous minor mergers and gas accretion. Adapted from Naab et al. (2014) with permission.

effects, are important. As the expected major merger rates are low, some massive galaxies might experience no major merger at all (see **Figure 1**). It is clear that galaxy mergers, in particular those of equal mass, can have a significant impact on galaxy kinematics and mass growth if they happen at late times. The importance of stars formed in merger-triggered starbursts may have been overestimated as well, particularly because most merger simulations ignored halo gas accretion. If halo accretion is included the disks have more realistic constant star-formation rates, and the contribution from merger-triggered star formation is significantly lower and sometimes negligible (Moster et al. 2011). This is supported by observations indicating that most star formation in the Universe happens in relatively normal morphologically settled disk-like galaxies (e.g., Daddi et al. 2007). Merging systems with enhanced star-formation rates seem to be of minor importance but might help in the transition to quenched early-type galaxies (Wuyts et al. 2011). Observations at low and high redshift also provide evidence that significant black hole accretion is not solely connected to merging but also to gas-rich, disk-like galaxies that can host AGNs of significant luminosity (Georgakakis et al. 2009, Cisternas et al. 2011, Schawinski et al. 2011, Kocevski et al. 2012). Also, cooling flow instabilities within the hot gas of elliptical galaxies lead to a secular branch of AGN fueling. Apparently major mergers can host luminous AGNs but by no means are all AGNs induced by mergers. Also it seems unlikely that the population of present-day early-type

galaxies can have directly formed via mergers among the population of present-day disk galaxies and their progenitors, as the early-type population is too old, too massive, and too metal rich (Naab & Ostriker 2009). At earlier times the discrepancy in mass and size between observed Milky Way progenitors and massive early-type galaxies is even more pronounced (Patel et al. 2013a).

1.6. Ranking and Matching

A fundamental question in galaxy formation, embedded in the modern hierarchical cold dark matter framework, is how much of the available baryonic matter is converted into stars in the central galaxies in dark matter halos. This quantity might be termed galaxy-formation efficiency or galaxy fraction $f_{\rm gal}$. There have been a number of attempts to estimate this number for the Milky Way. Whereas the stellar mass of the Milky Way is relatively well determined (Rix & Bovy 2013), the major uncertainty is in the mass of the Milky Way's dark matter halo. Typically mass estimates are in the range of $1–2 \times 10^{12}\,{\rm M}_\odot$ (Li & White 2008, Xue et al. 2008, Watkins et al. 2010, Bovy et al. 2012, Bland-Hawthorn & Gerhard 2016). The masses result in galaxy fractions of $f_{\rm gal} \sim 20–40\%$. With much better observed stellar mass functions at low and high redshifts and converged dark matter simulations for a given cosmological model, it has become possible to estimate the galaxy-formation efficiency (or the relation of galaxy mass to halo mass) for a large range of halo masses locally and at higher redshifts. The methods used include halo occupation distribution modeling (Berlind & Weinberg 2002, Bullock et al. 2002, Kravtsov et al. 2004), conditional luminosity function modeling (Yang et al. 2003), or a rank-ordered matching of observed galaxy mass functions to simulated halo mass functions (Vale & Ostriker 2004, 2006; Conroy et al. 2006; Shankar et al. 2006; Behroozi et al. 2010, 2013; Moster et al. 2010, 2013; Hearin & Watson 2013; Lu et al. 2015).

Most of these studies indicate that around 10–20% of the available baryons are converted into stars in dark matter halos of $\sim 10^{12}{\rm M}_\odot$. This fraction is lower in dark matter halos of higher and lower mass with considerable uncertainties at both ends (see, e.g., Gonzalez et al. 2013, Guo & White 2014, Kravtsov et al. 2014). The mismatch of most early cosmological simulations with these empirical estimates was highlighted by Guo et al. (2010), and galaxy fractions became a standard test presented in almost every publication about cosmological simulations. Also at higher redshift, the tension with simulations was formerly much more severe (see, e.g., Moster et al. 2013) owing to the overly efficient early conversion of baryons into stars.

The matching models also provide an independent estimate of the amount of stars formed in the galaxies (in situ star formation as measured by the star-formation rates) and the amount of stars accreted in galaxy mergers. The general conclusion is that all galaxies are dominated by in situ star formation at high redshift ($z \gtrsim 1.5$). This is a trend that continues to low redshift for moderate mass (Milky Way–type) galaxies that are predicted to have accreted between 5% (Moster et al. 2013) and 30% (Behroozi et al. 2013) of their stellar mass. High-mass galaxies assemble more and more of their stellar mass by mergers toward lower redshifts. However, the estimated fractions of accreted stars by $z = 0$ of galaxies in massive halos ($M_{\rm halo} \sim 10^{13}$) vary significantly between 20% and 60% (Behroozi et al. 2013, Moster et al. 2013, Yang et al. 2013). The general trend is similar to simulations (e.g., Oser et al. 2010, Gabor & Davé 2012, Lackner et al. 2012, Rodriguez-Gomez et al. 2016, Qu et al. 2017). It has also been highlighted that galaxies in massive halos ($M_{\rm halo} \gtrsim 10^{13}\ {\rm M}_\odot$) form their stars before the halo assembles. Low-mass galaxies form their stellar components after their halos assemble (Conroy & Wechsler 2009).

2. AB INITIO SIMULATIONS OF GALAXY FORMATION

2.1. Star Formation and Gas Cooling

Most modern cosmological galaxy formation simulations allow for metal enrichment and metal-dependent radiation equilibrium cooling (for specific implementations see, e.g., Kravtsov 2003, Scannapieco et al. 2005, Oppenheimer & Davé 2006, Tornatore et al. 2007, Ceverino & Klypin 2009, Wiersma et al. 2009, Vogelsberger et al. 2013) of gas in the presence of the UV/X-ray background radiation from quasars and galaxies (e.g., Faucher-Giguère et al. 2009, Haardt & Madau 2012). If the gas is cooling rapidly or in the presence of a rapidly changing radiation field, nonequilibrium cooling is more accurate (see, e.g., Gnat & Sternberg 2007, Oppenheimer & Schaye 2013b), and first steps in this direction have been made in galaxy-scale simulations (Oppenheimer & Schaye 2013a, Richings et al. 2014, Forbes et al. 2016, Hu et al. 2016, Oppenheimer et al. 2016, Richings & Schaye 2016). Out of the cool gas reservoir the formation of the stellar populations is modeled in a simplified way as the relevant spatial and temporal scales as well as the complex ISM physics cannot be resolved in a cosmological context.

Cosmological simulations typically treat star formation in a Schmidt-type manner (Schmidt 1959) relating the local star-formation rate density to the gas density divided by a timescale. This timescale depends on local gas properties like the dynamical and/or gas cooling time as introduced by Katz (1992) and Cen & Ostriker (1992b). Some implementations couple the star-formation rate to molecular gas properties inspired by observed connections (Wong & Blitz 2002, Kennicutt et al. 2007, Bigiel et al. 2008, Leroy et al. 2008, Kennicutt & Evans 2012) and use a constant timescale in combination with the variable local H_2 fraction (e.g., Pelupessy et al. 2006, Robertson & Kravtsov 2008, Gnedin et al. 2009, Christensen et al. 2012, Feldmann et al. 2012, Kuhlen et al. 2012, Monaco et al. 2012) which is, however, itself connected to the H_2 formation timescale. It should be noted that H_2-based star-formation models in galaxy simulations add another level of complexity and uncertainty. The small-scale structure of the ISM, the detailed radiation field, ionization degrees, and magnetic field strengths, all relevant for H_2 formation (e.g., Glover & Mac Low 2007, Hennebelle & Iffrig 2014, Walch et al. 2015), are unresolved in most galaxy-scale and all cosmological simulations (see, however, Hopkins et al. 2012b), and it is unclear whether H_2 formation is the primary driver for star formation (see, e.g., Glover & Clark 2012, Krumholz 2013).

The star-formation models typically require a normalization, the star-formation efficiency, as well as a parameter determining the scaling with gas density. The parameters are adjusted to match the zero point and the slope of the observed Kennicutt–Schmidt relation between star-formation rate surface density and gas surface density (Kennicutt 1998). The basic implementations have been extended by subresolution models to capture some characteristics of the multiphase structure of the gas (e.g., Springel & Hernquist 2003). An alternative implementation for star formation is based on gas pressure (see, e.g., Schaye & Dalla Vecchia 2008, Schaye et al. 2015), assuming that galactic disks are in approximate vertical pressure equilibrium. Such a model has been shown to be in good agreement with the observed Kennicutt–Schmidt relation with no need for additional calibration (Schaye & Dalla Vecchia 2008). If used in combination with a fixed equation of state for the star-forming gas, the behavior is similar to a density-dependent criterion, as the relation of gas pressure and density is fixed. In general, only gas below a certain temperature and above a certain density, which can be metal dependent, is eligible for star formation [see Hopkins et al. (2013b) for a discussion of star-formation criteria]. Also, in large-scale cosmological simulations these parameters must be calibrated as the ISM is in general unresolved, and gas cooling is effectively not followed below a few thousand Kelvins (Vogelsberger et al. 2014, Khandai et al. 2015, Schaye et al. 2015).

2.2. The Formation of Disk-Dominated Systems

Even though the formation of Milky Way systems has turned out to be the more difficult problem, it was historically the first one tackled. Can we make the Milky Way from reasonable cosmological initial conditions applying the relevant physical processes? Simulators typically have used the zoom technique (Navarro & White 1994), wherein a representative region of the Universe is simulated first with a dark matter only code, and then a relevant high-density piece is resimulated with a hydrodynamical code with allowance for the gravitational forces and gas inflow due to the surrounding matter.

In hierarchical cosmological models for the formation of galaxies, small structures form first, grow, and merge into larger objects. In this framework, galaxies form through the cooling of gas at the centers of dark matter halos, where it condenses into stars (White & Rees 1978). To match the observed properties of galaxies and galaxy clusters, purely gravitational processes on their own cannot account for cosmological structure formation, but gas cooling/dissipation processes must be considered. Three very early papers by Binney (1977), Rees & Ostriker (1977), and Silk (1977) presented the physical arguments for the observed scales of galaxies noted in our first paragraph. It had been realized early on from analytical estimates that the conservation of angular momentum of the cooling gas within dark matter halos could lead to the formation of galactic disks with flat rotation curves (Fall & Efstathiou 1980). Early work (White & Rees 1978) noted that at high redshift, gas has to be prevented from excessive cooling into overly dense regions—possibly by feedback from massive stars—to avoid the overproduction of condensed baryonic matter (Larson 1974, Dekel & Silk 1986, Navarro & Benz 1991). Also, to produce dynamically cold and thin stellar, extended disks, the accretion of high angular momentum gas from outer regions of the halos is needed in the more recent past (Fall 1979). This would require feedback processes to eject gas and avoid early over-efficient star formation at high redshift as well as the formation of gas reservoirs to allow the gas to return at low redshifts with higher angular momentum.

Early cosmological simulations including the dissipative gas component (but neglecting star formation) confirmed the problem (Katz & Gunn 1991, Navarro & Benz 1991, Navarro & White 1994). Too many baryons settled into disks that were much more compact than observed spiral galaxies with too-high rotation velocities due to substantial angular momentum loss during the assembly process caused by mergers. Not only was the angular momentum for the forming gaseous disks too low but also too many baryons would be locked up in galaxies (Navarro et al. 1995, Navarro & Steinmetz 1997).

The over-cooling problem was confirmed by many studies that followed (see, e.g., Balogh et al. 2001). Once a stellar component was included in the simulation it was possible to approximately treat the feedback from young stellar populations. In addition to radiative cooling the role of energy injection by supernovae could be tested. Investigators quickly discovered that, though the detailed implementation can change the results significantly (e.g., Navarro & White 1993, Sommer-Larsen et al. 1999, Thacker & Couchman 2000, Robertson et al. 2004, Okamoto et al. 2005), almost all cosmological simulations resulted in the overproduction of stars in low angular momentum bulges (e.g., Katz et al. 1996, Balogh et al. 2001, Kereš et al. 2005). It was again suggested that the origin of the problem lies at higher redshift (van den Bosch et al. 2002, D'Onghia & Burkert 2004). Galaxies would be less concentrated and have higher specific angular momentum if gas cooling were suppressed before the host halo has assembled (Weil et al. 1998). Still, simulations experimenting with thermal and kinetic energy injection [e.g., Abadi et al. (2003a) and many that followed] resulted in similar problems, with the conclusion that the assumed feedback models were insufficient to prevent the early collapse of low angular momentum baryons and their conversion into stars, a problem that remained unsolved for a long time.

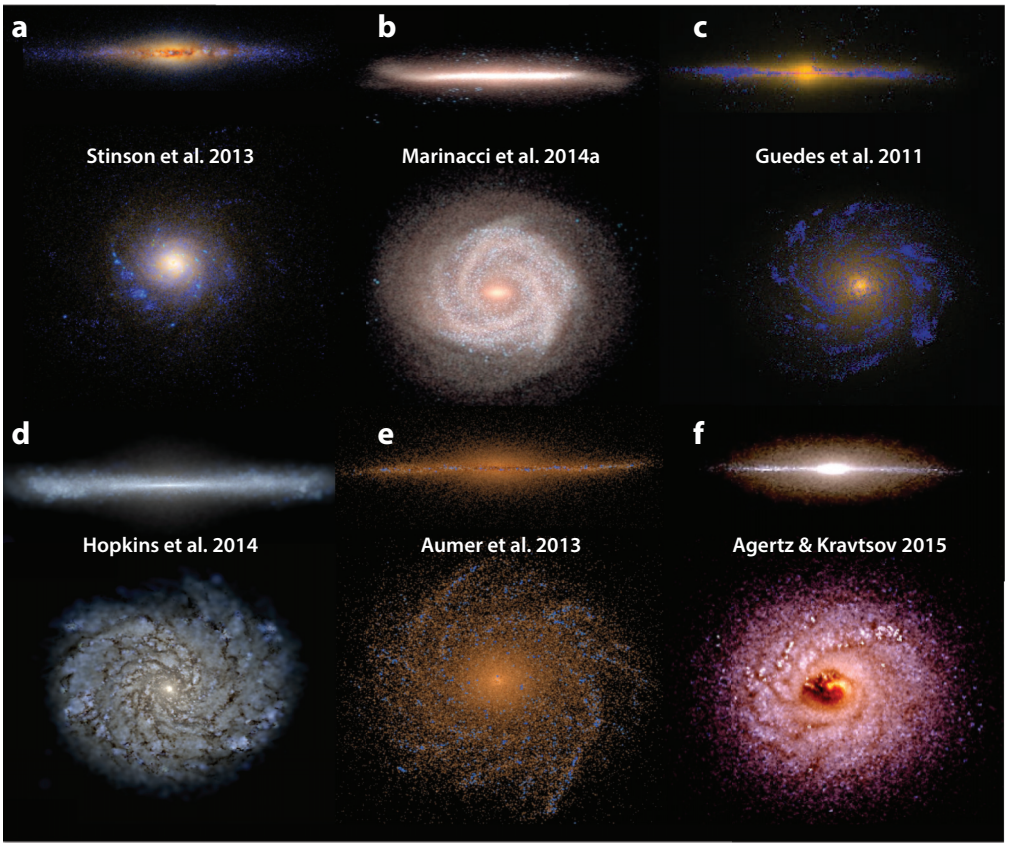

Figure 2

Recent cosmological zoom simulations with strong stellar feedback of galaxies with spiral-like morphologies. The pictures show mock images of the stellar light. (*a*) SPH (GASOLINE) simulation of Stinson et al. (2013) including dust attenuation. (*b*) Moving-mesh (AREPO) simulation of Marinacci et al. (2014a). (*c*) SPH (GASOLINE) simulation of Guedes et al. (2011). (*d*) SPH (GIZMO) simulation of Hopkins et al. (2014). Only the face-on view includes dust attenuation. (*e*) SPH (GADGET) simulation of Aumer et al. (2013). (*f*) AMR (RAMSES) simulation of Agertz & Kravtsov (2015). Only the face-on view includes dust attenuation. Abbreviations: AMR, adaptive mesh refinement; SPH, smoothed particle hydrodynamics.

Thus, the early attempts at ab initio cosmological computations failed or only partially succeeded to make disk systems that were as low-mass and extended in space and time of formation as those in the real Universe (Abadi et al. 2003a,b; Governato et al. 2004; Robertson et al. 2004; 2006a; Scannapieco et al. 2009; Agertz et al. 2011; Piontek & Steinmetz 2011). It is important to recall that observations had shown (see Section 1.1) that real, forming galaxies were embedded in strong gaseous outflows; these were missing from the simulations.

Recently, a number of groups have made significant progress on reducing the galaxy fraction, $f_{\rm gal}$, in halos of $\sim 10^{12}$ $M_\odot$ and at the same time forming spiral galaxies with more realistic properties. In **Figure 2**, we show examples from six groups who recently succeeded in producing disks with spiral-like morphologies but used very different simulation codes. These studies utilize a variety of qualitatively different subresolution approaches to the response of the high-density star-forming gas on newly formed and dying stellar populations. Commonalities to all these successful approaches are that gas in dense star-forming regions can efficiently be pushed out in a

galactic outflow and, possibly, escape from the galaxies and their dark matter halos. With outflow launching, Milky Way–like halos develop disk-like galaxies. Detailed investigations of gas flows in the forming galaxies—which are most easily followed in Lagrangian SPH simulations (see also Genel et al. 2013; Nelson et al. 2015, 2016)—have revealed most characteristics and consequences of galactic outflows. With strong stellar feedback, a significant fraction of the low angular momentum gas cooling to the centers of dark matter halos at high redshift is prevented from being converted into stars and can be blown out of the galaxies. When the protogalaxies are still small and have shallow potential wells, this gas leaves the galaxies and never returns or can return at much later times with angular momentum enhanced by nonlinear gravitational torques or mixing (e.g., Marinacci et al. 2011) with the rotating halo gas (Brook et al. 2011, Übler et al. 2014). The outflow suppresses the formation of stellar bulges from the low angular momentum gas at high redshift and enriches the circumgalactic medium with metals (Governato et al. 2010, Brook et al. 2012, Marinacci et al. 2014b, Christensen et al. 2016). It also reduces the previously reported dramatic effects of mergers. The gas still loses angular momentum but a significant fraction can be ejected before stars are formed. This is particularly efficient if the mergers happen early in smaller protogalaxies (Übler et al. 2014).

Contrary to what had been believed for a long time, even galaxies with early major mergers can evolve into present-day disk-like galaxies with low bulge fractions (Springel & Hernquist 2005, Robertson et al. 2006a, Aumer et al. 2014). For more massive systems the enriched gas is kept within the halo (in a galactic fountain) and is accreted back onto the galaxy later on with metallicity enhanced, sometimes repeatedly (Oppenheimer & Davé 2008, Oppenheimer et al. 2010, Pilkington et al. 2012, Brook et al. 2014, Genel et al. 2015). This process reduces star formation and delays the onset of galaxy formation in halos of all masses, in much better agreement with high-redshift abundance matching constraints (e.g., Hirschmann et al. 2013, Stinson et al. 2013, Hopkins et al. 2014). The late accretion of gas with high angular momentum from outside the halo is increased as fewer baryons were converted into stars in accreted structures. This is pretty much as it was predicted 38 years ago (Fall 1979).

In addition, at low redshift a moderately constant gas accretion rate onto spiral galaxies can be sustained by enriched gas that has been cycling within the halo of the galaxy (Oppenheimer et al. 2010, Übler et al. 2014, Christensen et al. 2016). Therefore gas accretion onto the galaxy is decoupled from the halo assembly, resulting in flatter star-formation histories more consistent with observations (Hirschmann et al. 2013, Stinson et al. 2013, Hopkins et al. 2014, Woods et al. 2014). In **Figure 3**, we show two recent examples of the generic effect of strong feedback on galactic star-formation rate histories. Additionally, Milky Way progenitor galaxies are larger (with strong feedback models), already at high redshift, and the overall cosmological evolution in size is significantly reduced (Hirschmann et al. 2013, Aumer et al. 2014) in much better agreement with observations. The above results rely on recipes to treat physical processes that are relevant below the resolution scale of the simulations and sometimes even impact the simulation in well-resolved regions. The variety of these models is remarkable, and a good understanding of the strengths and weaknesses of these models is relevant to assess whether scientific progress has been made or whether the good agreement with observations is the result of an empirical matching exercise. In the following, we review the general pathways followed by different groups.

Feedback from massive stars has long been suggested to resolve the over-cooling problem in galaxy formation, and various different subresolution feedback models have been presented to approximate the complex physical processes. Here, we call a subresolution model an empirical, physically motivated numerical recipe representing the large-scale impact of energy, mass, and momentum during the life and death of massive stars in state of the art cosmological simulations of large volumes. These models are necessary as the finest resolution elements (in large-scale

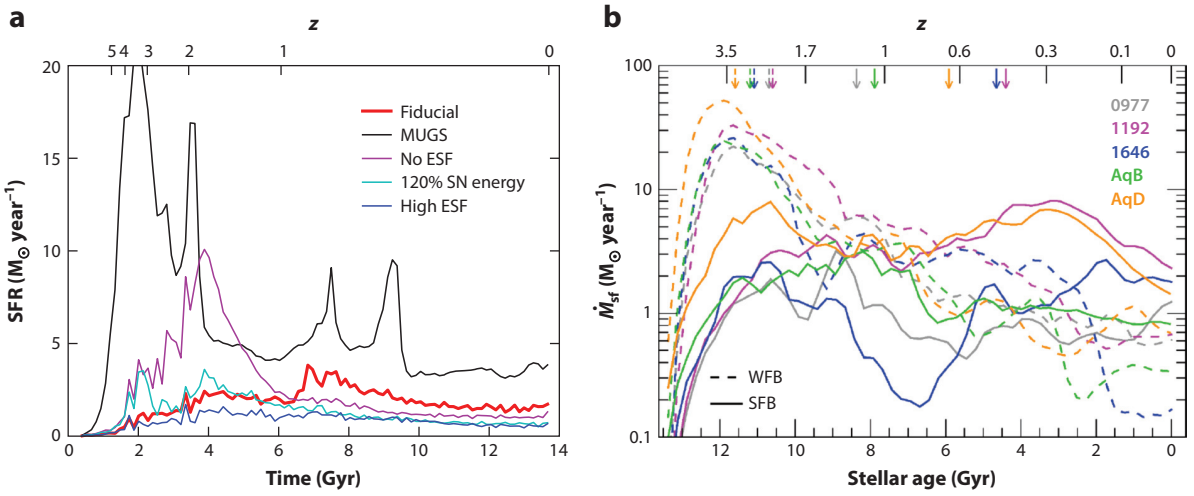

Figure 3

The effect of stellar feedback on the star-formation histories of simulated disk galaxies. Stronger feedback results in the suppression of early star formation, relatively flat star-formation histories and, in the cases shown here, disk-like morphologies. The flatter star-formation rate histories, but not the disk-like morphologies, are generic for all simulations with strong feedback. Flat star-formation histories are in better agreement with observations of Milky Way–sized spiral galaxies. (*a*) The simulations presented by Stinson et al. (2013) show peaked star-formation histories for simulations with weak feedback (MUGS, no ESF; Stinson et al. 2010). Star formation at high redshift is suppressed for models with strong feedback (fiducial, 120% SN energy, High ESF). (*b*) The same trend is seen in a comparison of five galaxies simulated with weak (*dashed lines*, Oser et al. 2010) and strong feedback (*solid lines*, Aumer et al. 2013). The stellar half-mass formation times (*arrows*) are shifted from $z \sim 2$ to $z \lesssim 1$ (Übler et al. 2014). Abbreviations: ESF, early stellar feedback; MUGS, McMaster Unbiased Galaxy Simulations; SFB, strong feedback; SFR, star-formation rate; SN, supernova; WFB, weak feedback.

cosmological simulations) are typically a few hundred parsecs, which makes it impossible for these simulations to capture the small-scale multiphase structure of the galactic ISM. In Section 3.1, we demonstrate why these models can only be a crude representation of reality, limiting the predictive power of present-day galaxy-formation simulations.

One class of models might be termed delayed cooling models (Gerritsen 1997, Thacker & Couchman 2000). In one incarnation of this approach (Stinson et al. 2006) the energy from supernova explosions is injected into neighboring gas, but the cooling is turned off for gas inside the expected Sedov blast wave radius (McKee & Ostriker 1977). This way gas can efficiently be heated and accelerated. Although often criticized as being unphysical due to the suppression of gas cooling, the model attempts to allow for formation of superbubbles [e.g., Mac Low & McCray (1988); see Keller et al. (2015) for a modern implementation of superbubble formation in cosmological simulations, and also see Section 3.1]. The delayed cooling model significantly reduces the galaxy stellar masses and promotes the formation of disk-dominated systems (Governato et al. 2007, Guedes et al. 2011, Keller et al. 2016). The models have been extended, in a simplified way, by taking into account the additional energy release from massive stars before they explode as supernovae (Stinson et al. 2013, Kannan et al. 2014, Wang et al. 2015). It has been pointed out by Rosdahl et al. (2017) that the delayed cooling approach results in a significant amount of thermally unstable circumgalactic gas, which can be problematic when estimating the gas emission and absorption in galactic halos.

A related approach is stochastic thermal feedback (Dalla Vecchia & Schaye 2012), which does not suffer from some of the problems of the delayed cooling approach (see, e.g., Rosdahl et al. 2017).

Here the mean thermal energy injection per unit formed stellar mass is fixed, and neighboring star particles are, stochastically, only heated if their temperatures can be moved above a certain temperature threshold (e.g., $\gtrsim 10^{7.5}$ K). This guarantees long cooling times, the onset of a Sedov phase, and efficient momentum generation similar to the delayed cooling models. The total energy injection is an adjustable parameter and can slightly exceed the available supernova energy (Crain et al. 2015, Schaye et al. 2015), compensating for the artificial overcooling. However, the model has been demonstrated to drive strong winds (Dalla Vecchia & Schaye 2012). It has been used for one of the most successful cosmological galaxy-formation simulation suites (the Eagle simulations, Schaye et al. 2015) in terms of matching observed galaxy population properties and their evolution with redshift (Furlong et al. 2015, Rahmati et al. 2015, Schaye et al. 2015, Bahé et al. 2016).

The gas cooling is also delayed in nonthermal heating models (Teyssier et al. 2013). Here the energy is injected into a nonthermal energy component, representing turbulence, magnetic fields, or CRs, with a dissipation timescale of ~10 Myr. The energy injection procedure follows the stochastic thermal heating (e.g., Roškar et al. 2014).

A two phase approach is followed by Scannapieco et al. (2006) where the hot and the cold gas phase are evolved separately using SPH (Marri & White 2003). The supernova energy added to a cold gas particle is stored (i.e., decoupled from the hydrodynamics) and only released when it can become a constituent of the hot phase. Accounting for the momentum input by supernovae and (potential) radiation pressure in a simplified way, this model also produces spiral galaxies with realistic properties (see **Figure 2**; Aumer et al. 2013).

Another popular approach might be termed wind feedback. Some fraction of the energy released by massive stars is injected into the surrounding gas in the form of energy or momentum by which it is driven away from the region of star formation. The wind is parameterized by a mass-loading factor η, i.e., the ratio of wind mass loss to the star-formation rate, and by a wind velocity $v_{\rm wind}$. The original implementation assumed a constant mass-loading and a fixed wind velocity coupled to a stiff effective equation of state for the gas resulting from thermal energy input from supernovae (Springel & Hernquist 2003). Here the gas in the wind is decoupled from the hydrodynamical calculations when leaving the star-forming regions with its given velocity and is later (the conditions depend on the respective implementations) incorporated in the calculations again (see also Vogelsberger et al. 2014). Observations and theoretical considerations, however, indicate decreasing mass-loading and increasing wind velocities in higher-mass galaxies with higher star-formation rates (Martin 2005, Murray et al. 2005). This motivated Oppenheimer & Davé (2006, 2008) to introduce a momentum-driven wind model. The wind velocity scales with the velocity dispersion of stars in the galaxies (or the dark matter; Vogelsberger et al. 2013) $v_{\rm wind} \propto \sigma$, the momentum input scales with the star-formation rate $\dot{m}_{\rm wind} \times v_{\rm wind} \propto \dot{m}_*$, and the mass-loading is inversely proportional to the velocity dispersion $\eta \propto {\rm d}m_{\rm wind}/{\rm d}m_* \propto 1/v_{\rm wind} \propto 1/\sigma_*$. Again, to ensure that the gas leaves the star-forming regions it is then decoupled and later re-incorporated in regions with lower gas density.

Although this model has become popular, some authors (Schaye et al. 2010) turned off the wind decoupling, the consequences of which are discussed by Dalla Vecchia & Schaye (2008). Although empirical in nature, the galactic wind models result in realistic (compared with observations) enrichment histories of galaxies and the circumgalactic medium (Finlator & Davé 2008, Davé et al. 2011), lower conversion efficiencies, particularly in the regime of disk galaxies (Sales et al. 2010, Puchwein & Springel 2013), reasonable abundances and flatter star-formation histories for low-mass galaxies and higher gas fraction for star-forming galaxies at high redshift (Oppenheimer & Davé 2008, Davé et al. 2011, Hirschmann et al. 2013), and a more realistic cosmic star-formation history (Schaye et al. 2010). Although originally developed for SPH simulations, decoupled momentum-driven winds have also been used in recent moving-mesh simulations with

wind velocities scaled to the local dark matter velocity dispersions (e.g., the Illustris simulation, Vogelsberger et al. 2014). With cosmological zoom simulations it has been demonstrated that realistic present-day spiral galaxies (Marinacci et al. 2014a, Grand et al. 2016) as well as gas-rich massive high-redshift disks (Genel et al. 2012, Anglés-Alcázar et al. 2014) can be formed with a momentum-driven wind model in which decoupling has been applied.

Alternatively, an energy-driven wind model has been proposed (Okamoto et al. 2010) to explain the low abundance of satellite galaxies in the Milky Way. Here the wind velocity also is assumed to scale with the velocity dispersion $v_{\rm wind} \propto \sigma$, the energy input scales with the star-formation rate $\dot{m}_{\rm wind} \times v_{\rm wind}^2 \propto \dot{m}_*$, and the mass-loading is taken to be inversely proportional to the square of the stellar velocity dispersion $\eta \propto {\rm d}m_{\rm wind}/{\rm d}m_* \propto 1/v_{\rm wind}^2 \propto 1/\sigma^2$. This model results in the same wind speeds but higher mass-loading for lower-mass galaxies and better agreement for the Milky Way satellites luminosity function (Okamoto et al. 2010). In a hybrid model Davé et al. (2013) combine a momentum-driven wind scaling with the energy-driven wind scaling for galaxies below $\sigma = 75$ km s^{-1} to obtain a better match to the galaxy mass function at low masses [see also Barai et al. (2013) for a radially varying wind model]. This transition was motivated by the idea that low-mass galaxies are more affected by supernova explosions, whereas the effect of radiation pressure takes over at higher masses (Murray et al. 2005, 2010). In an updated incarnation of the decoupled wind model Davé et al. (2016) used scaling from high-resolution cosmological zoom simulations (Muratov et al. 2015) to set the mass-loading and wind velocities. Efforts are underway to replace these heuristic methods with others based more closely on high-resolution multiphase physical modeling.

2.3. The Formation of Bulge-Dominated Systems

Spheroidal early-type galaxies have been easier to simulate from straightforward cosmological initial conditions (any cosmological simulation with weak feedback will result in the overproduction of spheroidal galaxies). The escape velocities are larger for these more massive systems and so the energy input from feedback matters somewhat less, and, though still important, stellar feedback appears to be less critical to the formation process. Empirically they are known to form in dense regions starting at early times, and the observed structures of protoellipticals are quite small as seen at redshift $z = 2$–3 (see Section 1.3). Thus, the difficulties encountered in making disk-like systems—too early star formation in too concentrated systems—are alleviated for the construction of physically plausible spheroidal systems. As a consequence, cosmological simulations with weak stellar feedback and without AGN feedback have effectively been used as reasonable initial models for the formation of massive, early-type galaxies. In these simulations the final galaxies follow observed early-type galaxy scaling relations of size and velocity dispersion with stellar mass (Naab et al. 2007; Feldmann et al. 2010, 2011; Oser et al. 2010; Johansson et al. 2012). They also have plausible stellar populations with metallicity distributions that are modulated by their merger history (Kobayashi 2004, 2005). However, compared with observations based on abundance matching constraints, their stellar masses are about a factor of 2–4 too high at a given halo mass (Oser et al. 2010). This is presumably due to the lack of sufficient energy input (see, e.g., Meza et al. 2003, Croton et al. 2006), and it has been alleviated as AGN feedback simulations have been improved.

For high halo masses, the evolution of the galaxies shows a clear two-phase characteristic (Naab et al. 2007, Feldmann et al. 2010, Oser et al. 2010, Johansson et al. 2012, Navarro-González et al. 2013, Rodriguez-Gomez et al. 2016, Qu et al. 2017). At early times ($z \gtrsim 1.5$) the galaxies grow by in situ star formation in the deep potential wells of massive halos. As the low angular momentum gas is efficiently converted into stars, some of the systems can be remarkably small (also supported

by mergers; Wuyts et al. 2010, Bournaud et al. 2011a), very similar to the population of observed high-redshift compact galaxies (Sommer-Larsen & Toft 2010; Oser et al. 2010; 2012; Wellons et al. 2016). Toward lower redshifts in situ star formation becomes less important as cold gas can no longer easily penetrate the shocked hot gaseous halos (e.g., Birnboim & Dekel 2003), and the mass assembly becomes dominated by the accretion of stars that have formed in other galaxies. Cosmological simulations clearly indicate that stellar accretion is more important at higher galaxy masses (Oser et al. 2010, Gabor & Davé 2012, Lackner et al. 2012, Rodriguez-Gomez et al. 2016, Qu et al. 2017). This robust trend is also found in abundance matching estimates (Section 1.6) and semianalytical galaxy-formation models (Khochfar & Silk 2006, Guo & White 2008), and it is strongest for central galaxies in galaxy clusters (Ostriker & Hausman 1977, De Lucia & Blaizot 2007). The late, collisionless assembly has important consequences for the structural evolution of the system. As a significant fraction of mass can be accreted in mergers with smaller and less-bound systems (Gabor & Davé 2012, Lackner et al. 2012), this stellar mass is added to the systems at large radii (Oser et al. 2010, Navarro-González et al. 2013, Rodriguez-Gomez et al. 2016, Qu et al. 2017). The resulting strong increase in galaxy size is driven by accreted stars. Simple arguments based on the virial theorem (Bezanson et al. 2009, Naab et al. 2009) show that the same mass added in many minor mergers will produce a much more extended galaxy than if that mass had been added in fewer, more major mergers (Equation 1, Section 1.5). Together with the weak decrease in velocity dispersion the evolution of the individual model galaxies is consistent with observational estimates.

The low present-day star-formation rates and spheroidal shapes of galaxies simulated with weak stellar feedback are primarily caused by the efficient early gas depletion and early conversion of gas into stars in combination with efficient shock heating of the halo gas and gravitational heating caused by the accretion of smaller systems (Khochfar & Ostriker 2008, Johansson et al. 2009b). Still, the weak feedback models provide an attractive start for the physical solution of the observed structural evolution of massive galaxies (see also Feldmann et al. 2011, Feldmann & Mayer 2015). In its extreme limit the assembly of brightest-cluster galaxies and the size evolution of cluster galaxies can be well explained in a substantially collisionless cosmological assembly model assuming that all stars in cluster progenitor galaxies have formed before $z \sim 2$ (Laporte et al. 2013).

Simulations neglecting AGN feedback have shown that the formation history of massive galaxies leaves its imprint on the gas and stellar kinematic properties of present-day early-type galaxies (Naab et al. 2014, Serra et al. 2014, Wu et al. 2014). Epochs dominated by gas dissipation result in the formation of flattened stellar distributions (disks), supported by rotation. Major mergers are rare, and during minor merger–dominated phases the stellar systems experience stripping and violent relaxation; existing cold gas may be driven to the central regions, causing starbursts, trigger the formation and growth of supermassive black holes, or be expelled from the systems in galactic winds. This, in turn, impacts the distribution of cold gas and the kinematics of stars forming thereof. With improved cosmological simulations we move toward a better understanding of the angular momentum evolution of galaxies (see Genel et al. 2015, Zavala et al. 2016). In a first step, using cosmological zoom simulations, Naab et al. (2014) have been able to demonstrate that gas dissipation and merging result in observable features (at present day) in the two-dimensional kinematic properties of galaxies, which are clear signatures of distinct formation processes.

Many of these features are in agreement with all the valuable predictions from isolated merger simulations (see Section 1.5). Dissipation favors the formation of fast-rotating systems and line-of-sight velocity distributions with steep leading wings, properties that can be directly traced back to the orbital composition of the systems [Röttgers et al. 2014; see also Bryan et al. (2012) for the orbital distribution of dark matter]. Merging and accretion can result in fast rotators or slowly

rotating systems with counter-rotating cores or systems with cold nuclear or extended (sometimes counter-rotating) disks showing dumbbell-like features all observed in real galaxies and in part well understood from binary merger experiments.

We have seen that models with stronger feedback and metal cooling, applied to cosmological simulations, delay the onset of star formation in more massive halos, and the systems become more gas rich at high redshift, a trend that continues toward low redshift. This makes galaxies too massive with too-high star-formation rates, particularly at the central regions (e.g., Kravtsov & Borgani 2012). This had also been found prior to cosmological simulations (e.g., Ciotti et al. 1991, Ciotti & Ostriker 1997), owing simply to the inevitable cooling flows occurring in massive systems. One-dimensional and two-dimensional high-resolution simulations of the effect of AGN feedback (Binney & Tabor 1995, Ciotti & Ostriker 2001, Sazonov et al. 2005, Novak et al. 2011) indicated that AGN feedback alleviates this problem. With ab inito cosmological simulations a number of groups have now demonstrated that feedback from an accreting supermassive black hole can suppress the residual star formation in the central regions of massive galaxies, confirming the proposal put forward by Silk & Rees (1998). In the following, we review some subresoluton approaches for implementing feedback from supermassive black holes.

Several different models have been proposed to approximate the effect of AGN feedback and to follow it in cosmological simulations. In most galaxy-scale subresolution models (starting from Springel et al. 2005b) the accretion rate onto the black hole $\dot{M}_{\rm BH}$ is computed based on the Bondi–Hoyle–Lyttleton formula (actually invented for spherical accretion of interstellar gas onto the Sun; Hoyle & Lyttleton 1939, Bondi & Hoyle 1944, Bondi 1952),

$$\frac{{\rm d}M_{\rm BH}}{{\rm d}t} = \alpha_{\rm boost}\frac{4\pi G^2 M_{\rm BH}^2 \rho}{(c_s^2 + v_{\rm rel}^2)^{3/2}}. \quad (2)$$

Here c_s is the sound speed of the surrounding gas and $v_{\rm rel}$ is the relative velocity of the black hole and the gas [see Rosas-Guevara et al. (2015) for modifications of the Bondi rate due to an assumed viscous accretion disk; see also Hopkins et al. (2016) for the possible failure of Bondi accretion in high-resolution simulations]. Also included in many models is an adjustable accretion boost factor $\alpha_{\rm boost}$, which can have values up to 100 in some implementations. The general motivation for using a boost factor is the low resolution of the simulations that are unable to follow the accurate multiphase gas structure near the black holes and therefore the accretion rates [see discussion by Booth & Schaye (2009)]. In fact many implementations use Bondi accretion in combination with a stiff equation of state for the high-density gas, resulting in gas with increasing temperature at higher densities—contrary to the expected structure in the dense ISM (McCarthy et al. 2010; Puchwein & Springel 2013; Vogelsberger et al. 2013, 2014; Hirschmann et al. 2014; Khandai et al. 2015; Schaye et al. 2015). As a result the sound speed becomes artificially high, and a high $\alpha_{\rm boost}$ compensates for this. From a practical, not physical, point of view the boost factor ensures that enough gas is accreted to grow supermassive black holes of reasonable masses. As shown by Springel et al. (2005b), the accretion in most models is limited by the Eddington rate. In some recent implementations (see, however, Pelupessy et al. 2007) the relative velocity between the black hole and the ambient medium is not considered (the Lyttleton part) as the black holes are continuously centered to the potential minimum of the host halo (e.g., Puchwein & Springel 2013, Vogelsberger et al. 2014). Choi et al. (2012) take an alternate approach that does not have a boost factor; they stochastically treat the overlap of the smoothing sphere and the Bondi sphere, thereby statistically allowing for the resolution limits. Also Schaye et al. (2015) have eliminated the boost factor and regulate the Bondi rate with the ratio of the Bondi-to-viscous timescale (Rosas-Guevara et al. 2015). Still, the same limitations apply for the temperature and density structure of the nuclear gas.

Shlosman et al. (1989) have proposed that black holes might be primarily fed by gas driven to the center by gravitational torques from nonaxisymmetric perturbations (see also, e.g., Bournaud et al. 2011b, Hopkins & Quataert 2011, Gabor & Bournaud 2013). Hopkins & Quataert (2011) argue that torque-driven accretion behaves qualitatively differently than other accretion models. The parameterized version of this accretion model is more complicated, making it less straightforward to include in larger-scale cosmological simulations, but the first attempts are promising and indicate that scaling relations can be recovered without the need for self-regulation (Anglés-Alcázar et al. 2013, 2017). Clearly the choice between the two approaches should be driven by the amount of angular momentum in the gas to be accreted; the torque-limited model should be preferred when the ratio of the centrifugal radius to the Bondi radius becomes larger than unity.

Approaches following the traditional feedback models assume that some fraction ($\epsilon_{\rm therm} \sim 0.05$) of the bolometric luminosity $L_{\rm bol} = \epsilon_{\rm r} {\rm d}M_{\rm BH}/{\rm d}tc^2$ (Shakura & Sunyaev 1973, Soltan 1982), with c being the speed of light and a radiative efficiency of $\epsilon_{\rm r} = 0.1$ (Shakura & Sunyaev 1973), is converted into and deposited as thermal energy in the surrounding ISM such that the energy injection rate is ${\rm d}E_{\rm therm}/{\rm d}t = \epsilon_{\rm therm}\epsilon_{\rm r}\dot{M}_{\rm BH}c^2$. Sijacki et al. (2007) proposed a jet bubble modification to this simple model that depends on the gas accretion rate onto the black hole. For accretion rates above 1% of the Eddington rate the usual fraction of $\epsilon_{\rm therm}\epsilon_{\rm r}$ of the accreted rest mass energy is deposited as thermal energy to the surrounding medium. For lower accretion rates the feedback efficiency is increased from 0.5% to 2% of the rest mass energy and is injected into heated off-center bubbles that can then buoyantly rise [see Fabjan et al. (2010), Hirschmann et al. (2014), and Vogelsberger et al. (2014) for slightly modified versions]. Such models are designed to mimic the observed jet-induced bubble formation (Fabian et al. 2006, Fabian 2012) and, due to the enhanced coupling efficiency at low accretion rates, i.e., low black hole growth rates (see, e.g., Churazov et al. 2005, Merloni & Heinz 2008), they help to prevent the formation of cooling flows and nuclear star formation in massive halos (Sijacki et al. 2007). Dubois et al. (2012), in a RAMSES implementation, also identify a radio mode at low accretion rates and inject kinetic energy into a jet-like bipolar outflow with a velocity of 10,000 km s^{-1} [see also Omma et al. (2004) and Brighenti & Mathews (2006) for the impact of jet feedback in isolated models].

Originally developed for SPH, the Sijacki et al. (2007) AGN feedback model has also been used in recent large-scale simulations with the moving-mesh code AREPO extended by the influence of the radiation field of the accreting black holes on the cooling rate of the gas (Vogelsberger et al. 2014, Sijacki et al. 2015). Here the effect of AGN feedback on reducing the galactic stellar masses was confirmed; however, it was at the cost of depleting the massive halos of gas due to the jet bubble feedback, inconsistent with observations (Genel et al. 2014). In general, these relatively straightforward models not only give reasonable galaxy and black hole masses at the high-mass end but they also result in plausible evolutions of the black hole populations and AGN luminosity functions across cosmic time (Puchwein & Springel 2013, Hirschmann et al. 2014, Khandai et al. 2015, Sijacki et al. 2015).

Instead of using a constant boost factor, Booth & Schaye (2009) scale $\alpha_{\rm boost}$ with the local density for high ambient gas densities and set it to unity for low densities—in combination with a stiff equation of state for dense gas [Schaye & Dalla Vecchia (2008); see Booth & Schaye 2009 for a detailed discussion]. The thermal feedback is regulated such that the black hole stores the energy until the surrounding particles can be heated to a certain high temperature (in this case $\gtrsim 10^8$ K), disfavoring rapid cooling of the gas and making the immediate feedback efficient by construction. The approach is similar to the stellar stochastic thermal feedback discussed in Section 2.2.1. It is clear that the density scaling of $\alpha_{\rm boost}$ makes the accretion more sensitive to the feedback, which in turn strongly affects the density. In general, however, the introduction of a temperature limit for the black hole feedback results in a stronger effect than in the Springel et al. (2005b) model

with no need for changing the energy conversion efficiency and the feedback methodology. This model also results in reasonable baryon fractions and stellar masses for massive galaxies and black hole masses (Schaye et al. 2015). In particular it reproduces reasonable gas fractions and X-ray luminosities for galaxy groups (McCarthy et al. 2010, Choi et al. 2014, Le Brun et al. 2014), which are over-predicted by models with a constant boost factor and thermal feedback.

An Eddington-limited thermal black hole feedback scheme similar to that of Booth & Schaye (2009), with a density dependent $\alpha_{\rm boost}$ and the same underlying equation of state for the gas, has also been implemented in the AMR code RAMSES (Teyssier et al. 2011, Dubois et al. 2012). The black holes are not seeded in halos above a certain mass, but the accreting sink particles are generated when certain conditions on the stellar component and gas density are met [Teyssier et al. (2011); see, e.g., Di Matteo et al. (2012), Dubois et al. (2012), Puchwein & Springel (2013), Hirschmann et al. (2014) for different implementations of black hole seeding].

Zoom simulations of group and cluster-sized halos in particular have highlighted the impact of AGN feedback on reducing the stellar mass in the central galaxies by preventing cooling flows and subsequent star formation (Sijacki et al. 2007, McCarthy et al. 2010, Teyssier et al. 2010). AGN feedback also has important consequences for the hot gas in these halos. By removing low-entropy gas at higher redshifts (at the peak of the black hole growth) AGNs bring the simulated present-day hot gas properties in much better agreement with observations of thermal X-ray emission (McCarthy et al. 2010, 2011; Le Brun et al. 2014).

The above simulations also indicate a potentially interesting effect of AGN feedback on the stellar kinematics. As the amount of gas cooling and subsequent star formation in the central galaxies is efficiently suppressed (Martizzi et al. 2012a, b), the ratio of in situ–formed to accreted stars is significantly reduced, increasing the size of the system but also reducing the amount of rotational support (Dubois et al. 2013, Martizzi et al. 2014). AGN feedback transforms brightest-cluster galaxies from fast rotators to slow rotators, possibly in better agreement with observations (Dubois et al. 2013, Martizzi et al. 2014). This highlights the potentially important role of AGN feedback for regulating the ratio of in situ star formation to accretion (Hirschmann et al. 2012, Dubois et al. 2013) determining the stellar kinematics of the systems and regulating the stellar density distributions.

The strength of these kinematic signatures will not only be influenced by feedback from AGNs and stars but also by the mass of the galaxies and their environment. Low-mass, star-forming disk galaxies favored in low-density environments predominantly grow by accretion of gas and subsequent in situ star formation; they are affected by stellar feedback and less so by AGNs. Higher-mass, early-type galaxies form in high-density environments—primarily affected by feedback from accreting supermassive black holes—and their late assembly involves merging with other galaxies, which might also be of an early type (e.g., Rodriguez-Gomez et al. 2016, Qu et al. 2017). So far it has not been possible to perform a statistically meaningful comparison of kinematic properties of galaxy populations to observed population properties, like the observed increasing fraction of slow versus fast rotators for early-type galaxies as a function of environmental density (Cappellari et al. 2011a). With the newly performed Eagle (Schaye et al. 2015) and Illustris (Vogelsberger et al. 2014) simulations this might now be possible for the first time, owing to the large simulated volume and the relatively high spatial resolution attained ($\lesssim$1 kpc). Not only can the simulated two-dimensional kinematic properties be compared with observations but it will also be possible to make (statistical) connections to characteristic formation histories and properties of progenitor galaxy populations and to investigate trends with environment. This will not only be limited to stellar kinematics but will also include gas kinematics and metallicity and two-dimensional stellar abundance patterns. In addition, we will be able to assess the impact of the major feedback mechanisms (from massive stars and AGNs) on the kinematic properties of high- and low-mass

galaxies in all environments, a study that will be supported by higher-resolution, cosmological zoom simulations for characteristic cases. Also several recent papers (e.g., Crain et al. 2010; Bogdán et al. 2013; Choi et al. 2014; Le Brun et al. 2014, 2015) have shown that a proper prediction of the thermal X-ray halos of massive galaxies provides a stringent test of the correctness of any implemented feedback scheme. We discuss mechanical and radiative AGN feedback models in Section 3.5.

3. THE NEED FOR ACCURATE MODELING OF THE GALACTIC INTERSTELLAR MEDIUM AND FEEDBACK

The large differences of subresolution models presented in the previous section are noteworthy but also a bit worrying as the models should be representations of the same underlying physical processes. Many groups have been able to design and calibrate feedback procedures that allow them to more or less successfully match the present-day galaxy mass function, or more accurately, the ratio of dark matter to galaxy masses, the cosmological evolution of galaxy abundances, and the evolution in galaxy sizes and stellar populations (the Eagle project seems to have done this most successfully). In **Figure 4** one can assess to what level the different groups have succeeded in making this calibration to present-day galaxy mass functions similar to the one presented by Li & White (2009). With the large conceptual differences in the respective feedback models the good (or not so good) agreement with the observed mass function can be attributed to a more or less successful tuning of the normalizations and scalings in the subresolution models. The theoretical predictions are stellar mass functions from large-scale cosmological simulations in recent publications: from Davé et al. (2013) using traditional SPH, energy- and momentum-driven decoupled winds, and a heuristic model for gas heating in massive halos (no AGN feedback); from Davé et al. (2016) using a meshless finite mass method with star-formation feedback scaling motivated by higher-resolution simulations and an improved empirical gas heating model to Davé et al. (2013) for massive halos; from Puchwein & Springel (2013) using traditional SPH with momentum-driven winds and thermal and bubble AGN heating; from Dubois et al. (2014) (Horizon-AGN) with AMR, mechanical supernova feedback, thermal AGN feedback with variable boost factor, and jet feedback for low accretion rates; from Vogelsberger et al. (2014) (the Illustris simulations) with a moving-mesh code, decoupled momentum-driven winds, thermal and bubble AGN heating, and radiation input from the AGNs; from Schaye et al. (2015) (the Eagle simulations) with improved SPH, stochastic thermal heating from stars and AGNs; from Hirschmann et al. (2014) (the Magneticum simulations) with traditional SPH, constant winds, thermal AGN heating, and a modified bubble heating; and from Khandai et al. (2015) (the MassiveBlack II simulations) with traditional SPH, decoupled wind, and thermal AGN feedback. The simulations have more or less succeeded in this exercise. For comparison, we show a (typical) observed galaxy mass function in the local Universe (Li & White 2009). Again, we point out that such a mass function is used for most simulations and alternative mass functions take extended stellar mass distributions in massive galaxies into account (Bernardi et al. 2013). Even with the significant differences in the subgrid model assumptions it seems that many simulations capture the basic characteristics. Still to be achieved are cosmological simulations yielding good matches to galaxy population properties on the basis of numerically resolved ab initio physical modeling of feedback processes.

Returning to the outline of the physical problems encountered in studying galaxy formation and evolution, we had already noted earlier that for problem B—feedback—there were a number of physical processes that we know are important but remain unsolved. Primary among them are the questions of which physical processes regulate the multiphase structure of the ISM and what is the main driver for galactic outflows.

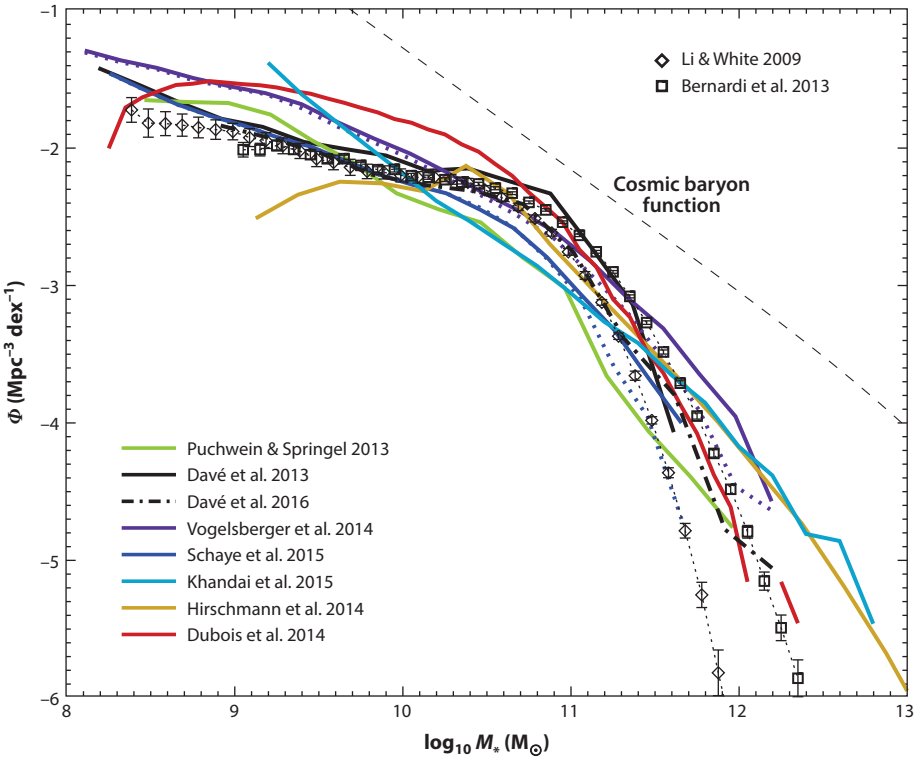

Figure 4

Comparison of galaxy stellar mass functions from recent large-scale cosmological simulations of representative volumes of the Universe. The simulations include stellar and AGN feedback with the exception of Davé et al. (2013), who use an empirical heating model in massive halos. The different groups typically adjust the key parameters in the varying subresolution models to match observations of galaxy mass functions like that of Li & White (2009). For reference, we show an alternative mass function with different mass estimates for massive galaxies (Bernardi et al. 2013). At a given mass the abundance can vary by up to an order of magnitude, still considering the range in spatial resolution (from 0.5 kpc to 3 kpc) and the significant difference in subresolution models, the agreement between the simulations is remarkable for some models. The dashed line for Vogelsberger et al. (2014) and Schaye et al. (2015) indicate different mass estimates. The dashed line shows the hypothetical galaxy mass function assuming the cosmic baryon fraction. Abbreviation: AGN, active galactic nucleus.

3.1. Supernova Explosions

Core-collapse supernova explosions have long been the primary suspect to play a crucial role in galaxy formation (Larson 1974, Dekel & Silk 1986, Navarro & White 1993). During these singular and final events in a massive star's life, typically 2–5 $M_\odot$ of gas are ejected into the ambient ISM at supersonic velocities of $v_{\rm eject} \sim 6{,}000$–$7{,}000$ km s^{-1} (Janka 2012), driving a shock into the ambient ISM. Apart from the injection of metals, supernovae can, in the energy conserving phase of the blast wave, heat about three orders more ambient mass than their ejecta to high temperatures. This makes them the prime sources of hot ($T \sim 10^6$ K) gas in the star-forming ISM. By creating the hot, X-ray–emitting phase they impact the large-scale multiphase structure of the ISM (McKee & Ostriker 1977, Li et al. 2015, Walch et al. 2015) and might be important for driving galactic outflows, fountain flows, and galactic winds through hot, low-density chimneys (Chevalier & Clegg

1985, Norman & Ikeuchi 1989, Heckman et al. 1990, Strickland & Stevens 2000, Heckman 2003, Joung & Mac Low 2006, Hill et al. 2012, Hennebelle & Iffrig 2014, Girichidis et al. 2016b). The momentum injected by supernovae contributes to the kinetic energy content of the ISM. With pure momentum injection simulations it has been argued that supernovae can create realistic turbulence [see reviews on ISM turbulence by Elmegreen & Scalo (2004) and Scalo & Elmegreen (2004)] in the warm and cold ISM and regulate the scale heights of galactic disks (by large-scale turbulent pressure) as well as their star-formation rates (see Ostriker & Shetty 2011, Kim & Ostriker 2015b).

The importance of supernova explosions for setting the ISM structure motivates a more detailed review of the different phases of supernova blast waves (see also Chevalier 1982, Cioffi et al. 1988, Ostriker & McKee 1988, Blondin et al. 1998, Draine 2011, Kim & Ostriker 2015a, Haid et al. 2016). The direct momentum of supernova ejecta is insufficient to accelerate a significant amount of gas to high velocities in the early free expansion phase. Once the supernova ejecta have swept up cold interstellar material of comparable mass the remnant enters the energy conserving Sedov–Taylor phase (Taylor 1950, Sedov 1959, Truelove & McKee 1999). In this phase about 1,000 times the ejecta mass is heated and about 10 times the initial (ejecta) radial momentum can be generated as long as the temperature changes are dominated by adiabatic expansion (this can amount to 100 times the ejecta momentum in the absence of cooling). As soon as radiative losses become dominant, a cooling shell forms, and the amount of hot gas decreases rapidly. Analytical estimates for the time $t_{\rm sf}$, radius $r_{\rm sf}$, velocity $v_{\rm sf}$, temperature $T_{\rm sf}$, mass $M_{\rm sf}$, and radial momentum $p_{\rm sf}$ at shell formation as a function of explosion energy E_{51} in units of 10^{51} ergs, and the number density of a homogeneous ambient medium in cm^{-3}, result in the following relations (taken from Kim & Ostriker 2015a, but see also Draine 2011):

$$t_{\rm sf} = 4.4 \times 10^4 \text{ years } E_{51}^{0.22} n_0^{-0.55}, \tag{3}$$

$$r_{\rm sf} = 22.6 \text{ pc } E_{51}^{0.29} n_0^{-0.42}, \tag{4}$$

$$v_{\rm sf} = 202 \text{ km s}^{-1} E_{51}^{0.07} n_0^{0.13}, \tag{5}$$

$$T_{\rm sf} = 5.67 \times 10^5 \text{ K } E_{51}^{0.13} n_0^{0.26}, \tag{6}$$

$$M_{\rm sf} = 1680 \text{ M}_\odot E_{51}^{0.13} n_0^{-0.26}, \text{and} \tag{7}$$

$$p_{\rm sf} = 2.17 \times 10^5 \text{ M}_\odot \text{ km s}^{-1} E_{51}^{0.93} n_0^{-0.13}. \tag{8}$$

Kim & Ostriker (2015a) have shown in detail that these analytic estimates agree well with direct, high-resolution, three-dimensional numerical simulations (see also Iffrig & Hennebelle 2015, Martizzi et al. 2015, Walch & Naab 2015).

After shell formation the supernova enters a short transition phase, and the following pressure-driven snowplow phase is powered by the homogeneous pressure inside the shell. Once all excess thermal energy is radiated away, no radial momentum can be generated anymore, and the remnant enters the momentum-conserving snowplow phase. Traveling into the ISM the shock wave transforms into a sound wave (when the expansion velocity reaches the sound speed of the ISM) and fades away. It can be shown that for Solar Neighborhood conditions an initially uniform medium will be completely changed within 2 Myr by overlapping remnants in their fade-away stage (Draine 2011). This simple argument indicates that supernovae alone might determine the thermal and dynamical state of the ISM (McKee & Ostriker 1977). Subsequent to this phase supernova remnants (SNRs) propagate in the multiphase medium with greater efficiency and reduced losses. These properties have yet to be fully assimilated into cosmological simulations of galaxy formation.

Radiative cooling, i.e., the actual ambient density and metallicity at the time of the supernova explosions, determines the duration of the momentum-generating phases of which the Sedov–Taylor phase is the most important. For single supernovae exploding in ambient densities of

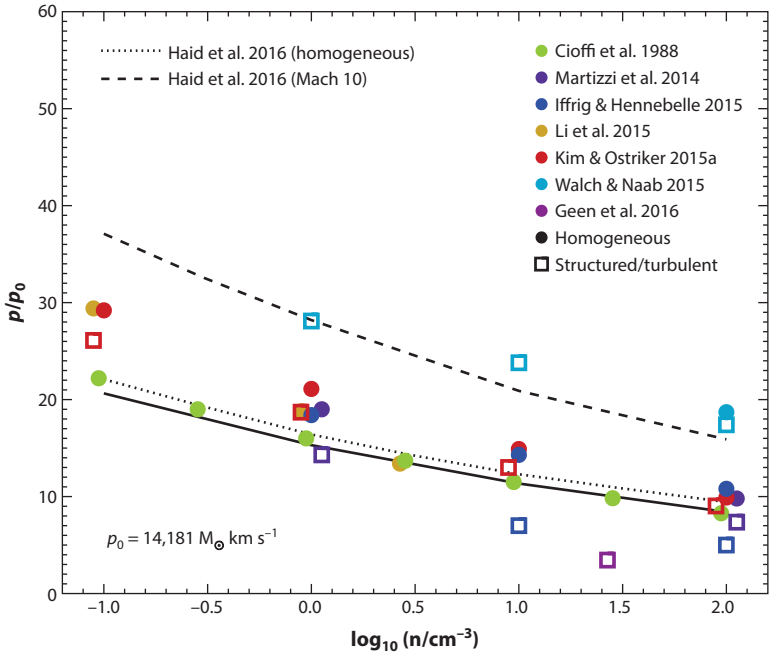

Figure 5

Momentum generated in radiative supernova remnants for various ambient densities normalized by a fiducial initial momentum of $p_0 = 14,181\ M_\odot$ km s^{-1} for an explosion energy of 10^{51} erg and two solar masses ejecta. The analytically derived momentum at shell formation (Equation 8, *solid line*) terminates the energy conserving Sedov–Taylor phase (Kim & Ostriker 2015a) and the momentum can increase a bit more until the beginning of the momentum conserving snowplow phase (*dotted line*). The dashed line indicates the momentum injection for an analytical model of a log-normal (Mach 10) density distribution (Haid et al. 2016). Colored symbols show results from three-dimensional numerical simulations (with the exception of the one-dimensional simulations by Cioffi et al. 1988) with homogeneous, structured, or turbulent ambient media carried out with three different grid codes and a particle-based smoothed particle hydrodynamics code.

$\sim 100 - 0.1$ cm^{-3} cooling becomes dominant after $\sim 10^4$–$10^{5.5}$ years, limiting the momentum generation to factors of ∼10–30 (Haid et al. 2016). For reliable simulations of the galactic ISM it is important that the momentum-generating phases of SNRs be captured accurately. Although analytic estimates are useful for homogeneous ambient media they cannot simply be applied to the more complex multiphase structure of a realistic ISM. Here, numerical simulations have made significant progress in recent years. We discuss this effort in a bit more detail as we think it is a good example of how resolved numerical simulations with different simulation codes can be used to understand a specific relevant physical process in more complex environments.

In **Figure 5**, we show an overview of mostly three-dimensional numerical simulations measuring the momentum injection into the ISM for the various conditions of the ambient ISM. Martizzi et al. (2015) have used the AMR code `RAMSES` for homogeneous ambient medium and one with a lognormal density distribution representing a Mach 30 turbulent ISM. The simulations of Kim & Ostriker (2015b) have been performed with the `ATHENA` code for a homogeneous and a structured two-phase medium (cold and warm phase). Additional simulations for a three-phase medium have been performed by Li et al. (2015) with the AMR code `ENZO`. We have to note that even at low resolution the total momentum input of a supernova can be correctly computed. However, the swept-up mass and the velocity of the shell can still be incorrect (Hu et al. 2016).

A supernova does not only inject momentum into the ISM. It also generates hot gas in the early phases of the remnant's evolution. The maximum amount of hot gas is reached at the time of shell formation, marking the end of the Sedov–Taylor phase. If no other supernova explodes within the remnant's radius until the time of shell formation t_{sf}, the remnant cools rapidly and no stable hot phase can be generated. For a homogeneous ISM of density n_0 and a given supernova rate density S, we can estimate the expectation value N_{hot} for a supernova to explode in a hot phase within the shell-formation radius r_{sf}:

$$N_{hot} = S\frac{4\pi}{3} r_{sf}^3 t_{sf}. \quad (9)$$

With Equations 4 and 7 this results in

$$N_{hot} = S2.13 \times 10^{-6}\ \mathrm{kpc}^3\ \mathrm{Myr}\ E_{51}^{1.09} n_0^{-1.81}. \quad (10)$$

For a typical gas surface density similar to the Solar Neighborhood of $10\,M_\odot\,pc^{-2}$ the Kennicutt relation (Kennicutt 1998) gives an observed star-formation rate surface density of $7 \times 10^{-2}\,M_\odot\,year^{-1}\,kpc^{-2}$. With a Salpeter-like initial mass function and an assumed disk thickness of 250 pc the resulting supernova rate density is $S \sim 280\,kpc^{-3}\,Myr^{-1}$. For an average gas number density of $n_0 = 1 cm^{-3}$ the expectation value would be only $N_{hot} \sim 6 \times 10^{-4}$. Due to the strong power-law dependence on the density in Equation 10 a lower density of $n = 0.015\ cm^{-3}$ results in $N_{hot} \gtrsim 1$, and a stable volume filling hot phase can form. Once such a condition is reached and the system cannot vent the hot gas it will undergo a thermal runaway. Subsequent supernovae explode in even hotter- and lower-density regions with even less thermal losses and larger shell-formation radii. Once the volume is dominated by over-pressured hot gas no shell will form, cooling losses are minimal, and most of the mass is in small cold clumps. This process has recently been described by Gatto et al. (2015) and Li et al. (2015) with hydrodynamical simulations in periodic boxes. If the ISM can vent the hot gas, an outflow is driven.

The strong dependence of the hot gas volume filling fraction in Equation 10 on the environmental density of the supernova explosions has significant consequences for the evolution of the galactic ISM. In **Figure 6**, we illustrate this with three numerical experiments (part of the Simulating the Life Cycle of Molecular Clouds (SILCC) simulation project; Walch et al. 2015). The setup is a stratified galactic disk with a surface density of $\Sigma_{gas} = 10\ M_\odot\ pc^{-2}$ embedded in a stellar disk potential. The initially homogeneous ISM is driven by supernova explosions at a constant rate based on observational estimates. If all supernovae explode at the current density peaks (typical densities of $n = 100\ cm^{-3}$; see Girichidis et al. 2016b), the explosions suffer from radiative losses, no hot phase develops, and the impact is limited to momentum injection. Rapidly a turbulent, pressure-supported two-phase (warm and cold gas) medium develops, and the scale height is set by the turbulent pressure. Draine (2011) presents a simple estimate for this process to take only 2 Myr. This behavior is reported from pure momentum injection models (Ostriker & Shetty 2011; Kim et al. 2011, 2013; Kim & Ostriker 2015b). The major shortcomings of these models are that no hot phase can develop and the cold phase cannot become dense enough for molecular gas formation (see, e.g., Walch et al. 2015). If some half of the supernovae do not explode in density peaks but rather at random locations in the disk, as would be expected from the number of early-type runaway stars discussed below, the ambient density distribution for supernovae becomes bimodal. Random supernovae in low-density regions $n \sim 0.1\ cm^{-3}$ compress the cold gas to higher densities $n \gtrsim 100\ cm^{-3}$, where the peak supernovae explode. The system can form a hot phase (see **Figure 6*b*,*e***). Once all supernovae explode at random positions (most ambient densities $n \lesssim 0.1\ cm^{-3}$), the ISM becomes highly structured and rapidly develops a stable hot phase, which expands into the halo and drives a galactic outflow [see Girichidis et al. (2016b) for the models

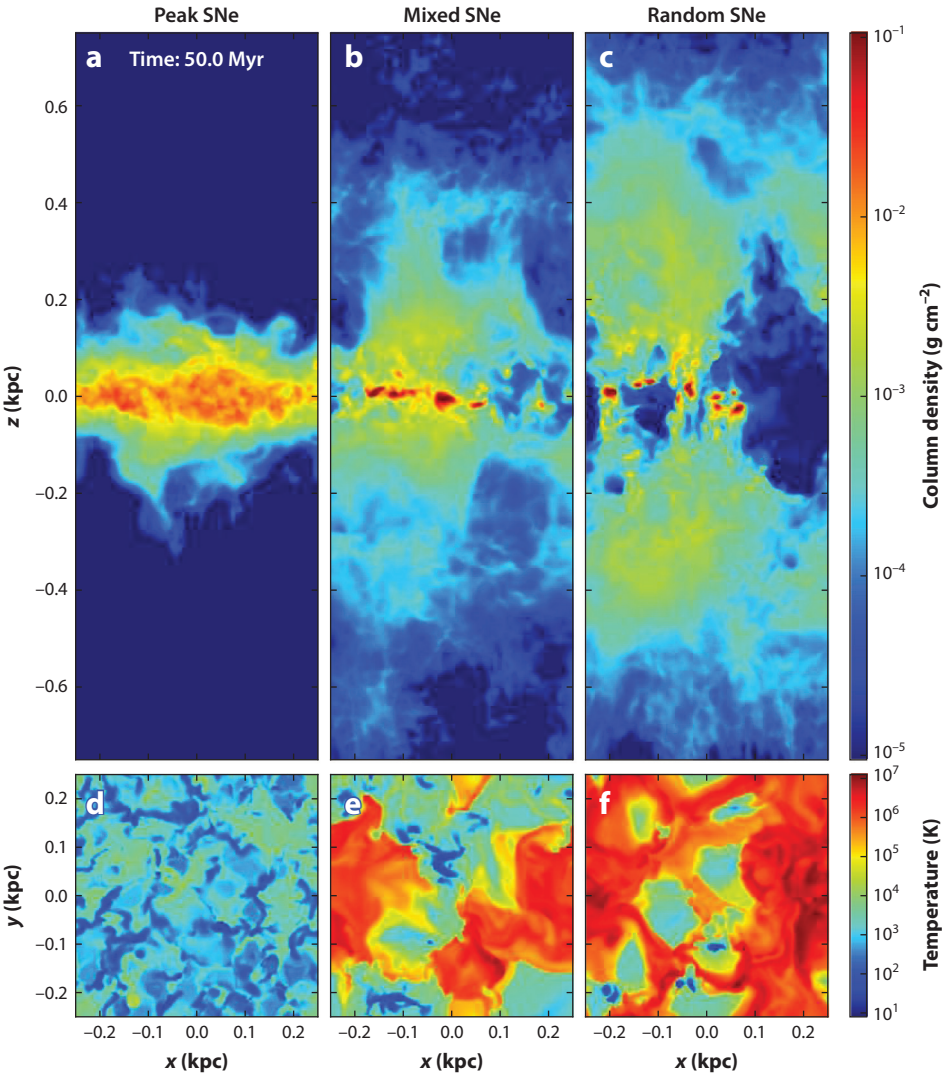

Figure 6

(*a–c*) Snapshots of the vertical gas column–density distribution and (*d–f*) midplane temperatures for three simulations of stratified galactic disk ($\Sigma_{gas} = 10\,M_{\odot}$ pc^{-2}) shaped by SNe exploding at a constant rate (data taken from the SILCC simulations; Walch et al. 2015, Girichidis et al. 2016b). (*a*,*d*) In peak SNe each supernova explodes at the current density peak. Rapid thermal losses limit the SN impact to momentum ejection, driving an (unrealistic) turbulent two-phase medium with no outflows and no hot gas. (*b*,*e*) With 50% of the supernovae exploding at random positions at lower densities a hot phase appears. (*c*,*f*) If all SNe explode at random positions the hot phase becomes volume filling and drives a vertical outflow (see Girichidis et al. 2016b). This figure clearly illustrates the strong impact of the actual location of SN explosions on the multiphase structure of the ISM and the driving of outflows (see Equation 10). We note that none of these variations can be captured in current large-scale cosmological simulations that have single-resolution elements of the size of the above simulation boxes (∼500 pc) and rely on subresolution models. Abbreviations: ISM, interstellar medium; SILCC, Simulating the Life Cycle of Molecular Clouds simulation project; SN(e), supernova(e).

shown in **Figure 6**]. This behavior has already been reported by pioneering three-dimensional hydrodynamical simulations of stratified disks by Korpi et al. (1999), de Avillez (2000), de Avillez & Breitschwerdt (2004), and Joung & Mac Low (2006). The major shortcomings of these types of models are that they neglect the galactic environment (radial gas flows and inflows) and, due to the idealized geometry, gas flows into and out of galactic halos cannot be modeled accurately (see, e.g., Martizzi et al. 2016).

OH maser measurements indicated that only about 15% of core-collapse supernovae interact with dense molecular gas (Hewitt et al. 2009). Therefore the typical ambient density for explosions is lower than that of the dense birthplaces of massive stars. Now the question is which astrophysical processes determine the ambient densities of supernova explosions? There are two phenomena that can result in this: The massive stars move away from their dense birthplaces into gas with lower volume densities and larger volume filling fractions and/or the stars change their environmental densities by stellar winds, ionizing radiation, and clustered supernova explosions.

Most, if not all, stars form in star clusters and are expected to be temporally and spatially correlated, eventually driving superbubbles with more efficient energy coupling and momentum generation (e.g., Mac Low & McCray 1988, Joung & Mac Low 2006, Sharma et al. 2014). The typical velocity dispersion in newly born star clusters is $\sim$1 km s^{-1} or 1 pc Myr^{-1}. Assuming the cluster becomes unbound, massive stars can travel up to 40 pc before they explode (assuming typical supernova delay times for single stellar populations). These walkaway stars can therefore easily leave their dense birthplaces and explode in lower-density regions. As most of the volume of the ISM is not in the cold phase, most supernovae might explode in the warm or hot phase, significantly changing the coupling efficiency (Slyz et al. 2005, Ceverino & Klypin 2009). There is also the runaway star population (Gies & Bolton 1986) (about 45% of O stars and 15% of B stars are runaways) with typical velocities of $\sim$30–40 km s^{-1} and maximum velocities as high as a few hundred kilometers per second (e.g., Silva & Napiwotzki 2011). These high-velocity stars originate from close binary systems becoming unbound by a supernova explosion (Zwicky 1957, Blaauw 1961) and/or from dynamical interactions in dense regions of star clusters (Poveda et al. 1967). They can travel up to several hundreds of parsecs away from their birthplaces far into interarm regions or the lower galactic halo. Their explosion locations in galactic disks can therefore be considered as almost random, similar to the explosions of type Ia supernovae, which contribute about 20–25% to the supernova rate in the Solar Neighborhood (Tammann et al. 1994). They explode independently of the gas mass distribution within the ISM, a process approximately taken into account in high-resolution simulations of stratified disks that are most useful to study the launching of outflows and, at the same time, create a realistically structured ISM (e.g., de Avillez & Breitschwerdt 2005, Joung & Mac Low 2006, Hill et al. 2012, Li et al. 2017). Such detailed small-scale simulations with a realistic ISM structure will help to bridge the gap in scale and physical understanding to galaxy-scale simulations.

3.2. Stellar Winds

Massive stars themselves also impact their ambient medium. Radiation-driven stellar winds from O and B stars (Castor et al. 1975, Puls et al. 1996, Kudritzki & Puls 2000) create bubbles of low-density gas around the stars. Typical B stars with masses $\sim$9 $M_\odot$, mass-loss rates of $\dot{M}_{\rm wind} \sim 10^{-9}$ $M_\odot$ year^{-1}, and wind velocities of $v_{\rm wind} \sim$ 2,000 km s^{-1} have an integrated wind luminosity of only a few times $\sim 10^{47}$ erg. However, very massive stars can reach as much as $E_{\rm wind} \sim 10^{51}$ erg. Although energetically much less important than supernova explosions, stellar wind–blown bubbles can significantly reduce the gas densities around massive stars and thereby increase the impact of the supernovae. Furthermore, because momentum injection goes as $\dot{E}/v$,

winds from massive stars can contribute more direct momentum than the supernovae themselves. Interestingly, stellar winds can also significantly reduce the star-formation process in forming star clusters [Dale & Bonnell (2008); although Dale et al. (2013, 2014) argue that the combined effect of stellar winds and ionizing radiation only has modest impact on star formation] and might be a stronger regulator for galactic star formation than supernovae (Gatto et al. 2017).

3.3. Radiation

Stellar evolution models indicate that the total energy released by newly formed stellar populations is, by a large margin of two orders of magnitude, dominated by stellar radiation, which itself is dominated by massive stars (e.g., Leitherer et al. 1999). By the time the first supernova, with a canonical energy of 10^{51} erg, has exploded, the stars would have already emitted $\sim 10^{53}$ erg as radiation, and $\gtrsim 10^{50}$ erg in stellar winds. It has been realized lately that, in galaxy-scale simulations, accounting for the stellar luminosity (and winds) might significantly enhance the coupling of the stellar energy and momentum output to the ISM (e.g., Hopkins et al. 2011, 2012c; Agertz et al. 2013; Roškar et al. 2014). The generation of momentum is of particular interest as it cannot easily be radiated away like thermal energy. The efficient cooling results in only a moderate 10% contribution of the thermal energy density in the ISM (Boulares & Cox 1990). Due to the generally severe radiation losses in dense interstellar environments it is, however, unclear, how much of the injected energy can be converted into momentum. If this process is efficient, then stellar radiation might significantly contribute to the driving of turbulence and the launching of galactic winds (e.g., Murray et al. 2005, 2010, 2011; Agertz & Kravtsov 2015; Geen et al. 2015).

Ionizing UV photons create HII regions around young massive stars by heating the parental cloud from $\lesssim 100$ K to $\sim 10^4$ K. At this stage the dynamics of the ISM is dominated by the thermal pressure of the ionized gas with sound speeds $\lesssim 10$ km s^{-1}. The momentum input by direct absorption of UV photons (single scattering) seems subdominant (Mathews 1969, Spitzer 1978, Arthur et al. 2004, Krumholz & Matzner 2009, Sales et al. 2014). It might be sufficient to drive turbulence at a low level (Gritschneder et al. 2009) and even disrupt small clouds on short timescales (Krumholz et al. 2006, Walch et al. 2012); however, overdense regions of the surrounding ISM will also be compressed into clumps and pillars (Dale et al. 2007, Gritschneder et al. 2010, Walch et al. 2012), making further coupling more difficult.

A full radiation transfer treatment of ionizing radiation from massive stars in galaxy-scale simulations is technically challenging [see, e.g., Wise et al. (2012) for single scattering]. It has been approximated in a Strömgren approach, i.e., the ISM around massive stars corresponding to a Strömgren sphere (Strömgren 1939) is ionized and heated to $\sim 10^4$ K (e.g., Hopkins et al. 2012c, Renaud et al. 2013) or in the optically thin regime (assuming escape fractions from clouds) with radiation field attenuation to follow the impact on gas cooling (e.g., Kannan et al. 2014). Kannan et al. (2014) claim a significant impact of the local UV radiation resulting in a suppression of star formation for Milky Way–like galaxies ($\sim$40%) by increasing the cooling time and the equilibrium temperature.

It has been argued that the radiation pressure on dust of re-emitted and scattered IR radiation can result in a significant momentum input into the ISM,

$$\dot{P}_{\rm rad} \sim (1 + \tau_{\rm IR}) L/c\,. \tag{11}$$

The efficiency of this process depends on the optical depth to the reradiated long-wavelength emission of the dust, $\tau_{\rm IR}$, i.e., on the details of multiple scatterings in optically thick regions surrounding the young stars. Based on small-scale simulations, Krumholz & Thompson (2013) argue that the momentum input does not exceed L/c owing to the structure, and therefore inefficient

trapping, developing in the ISM (Krumholz & Thompson 2012). However, using a different radiation transport method, Davis et al. (2014) find a slightly stronger coupling of the radiation. In an attempt to approximately include this effect in high-resolution galaxy-scale simulations Hopkins et al. (2011, 2012b, c) add momentum to the surrounding gas either in a stochastic or continuous way and indicate that they can use this process to drive galaxy-scale winds. Hopkins et al. (2011) give the gas particles initial kicks of the order the escape velocity from local gas clumps or star clusters (between 60 km s^{-1} and $\sim$350 km s^{-1} for clusters with masses $\sim 10^5$–$10^9\,M_\odot$), guaranteeing that dense regions become unbound before additional radiation pressure and supernovae can act. Locally they approximately compute τ_{IR} from the local gas properties assuming a high dust opacity of $\sim$5 cm^2 g^{-1} (see also Roškar et al. 2014) and use a model for attenuated radiation to compute the momentum input from all stars at large distances (Hopkins et al. 2011). This empirical implementation of radiation pressure may result in large-scale galactic winds by a nonlinear interaction of the different feedback mechanisms with the wind mass–loading changing as a function of galaxy properties (Hopkins et al. 2012c).

Other groups have followed similar paths to account for the full energy input of stellar populations and approximate the effect of radiation pressure. Agertz et al. (2013) have implemented the local momentum input as in Equation 11 with photon trapping acting at early ($t \lesssim 3$ Myr) embedded stages. Aumer et al. (2013) assume a large, fixed value for the optical depth ($\tau_{IR} \sim 25$) and scale the momentum input with the local gas velocity dispersion and metallicity. In a cosmological context it has been demonstrated, using different codes, that such efficient momentum input and the resulting winds can promote the formation of disk galaxies with appropriately low conversion efficiencies (Hopkins et al. 2014, Agertz & Kravtsov 2015; see **Figure 2**). However, Roškar et al. (2014) implemented an approximate radiation transfer for UV and IR radiation, where the dust opacity becomes an important factor to regulate the feedback efficiency. They argue that the momentum input required to drive strong outflows at the same time disturbs the gas and the resulting stellar disk so much that it becomes impossible to retain the flat disk morphology. In summary, though many promising calculations have been made [see, e.g., Rosdahl et al. (2015) for a first application of radiative transfer processes in galaxy-scale simulations], it is not yet clear how much radiation from young stars can really contribute to the driving of strong galactic outflows (see a first implementation of radiation transfer in ISM simulations in Peters et al. 2016). For a complete understanding of this process more accurate models for dust evolution in galaxy-formation simulations have to be considered. Good steps forward have been recently made in this direction (e.g., Bekki 2015, McKinnon et al. 2016, Zhukovska et al. 2016).

3.4. Magnetic Fields and Cosmic Rays

Magnetic fields and CRs, relativistic high-energy particles, mostly protons and electrons, are an integral, nonthermal component of the ISM. In the Solar Neighborhood the energy density in CRs, magnetic fields, and the kinetic energy density are comparable and significantly higher than the thermal pressure (Boulares & Cox 1990, Ferrière 2001). CR spectra have been measured over many orders of magnitude from $E_{CR} \sim 10^7$ eV up to the energies of $E_{CR} \sim 10^{20}$ eV. As the galactic CR energy spectrum is rather steep with $P \propto E^{-2.7}$ the majority of the energy is deposited at lower energies with a peak at around a few gigaelectronvolts, which is the expected range of significant dynamical impact of CRs on the ISM within a star-forming galaxy. The main acceleration mechanism for galactic CRs, in particular those below the knee in the CR spectrum, is considered to be diffusive shock acceleration (see, e.g., Bell 1978, Blandford & Ostriker 1978) and nonlinear diffusive shock acceleration (Malkov & O'C Drury 2001) in shocks of SNRs [see Hillas (2005) for a review, and recent observations by Ackermann et al. (2013)]. Although both

electrons and protons are accelerated in strong shocks, the protons carry most of the energy stored as CRs.

The fraction of energy generated in supernova shocks is highly uncertain, and this process can, of course, not be simulated in galaxy-scale simulations. The estimates mostly range between 5% and 30% of the total supernova explosion energy (Kang & Jones 2006, Ellison et al. 2010) with increasingly fundamental, ab initio calculations now being made (e.g., Caprioli et al. 2015). If a significant fraction is stored in CRs—which cool much slower than thermal gas by hadronic interactions and Coulomb and ionization losses—they can be carried over large distances and significantly impact the ISM, provided the coupling between CRs and the thermal gas is strong enough (e.g., Breitschwerdt et al. 1991, Zweibel & Heiles 1997). CRs diffuse from the shocks and, later on, stream through the ISM. The bulk of CRs may be trapped at first by scattering by self-excited Alfvén waves, which causes a slowed-down outward diffusion and additional momentum transfer to the gas (Caprioli et al. 2015). Once the CRs are able to escape the SNR, a streaming instability is excited if the necessary conditions for the dynamical coupling between the CRs and the gas are met (i.e., a large-scale CR gradient toward the galactic halo is required; Kulsrud & Pearce 1969), effectively transferring CR energy and momentum to the thermal gas. In addition the CRs exert a pressure on the thermal gas by scattering off Alfvén waves. It is therefore expected that CRs have a significant impact on the thermal and dynamical properties of the ISM. The propagation of CRs through the ISM is complex and often approximated by diffusion with coefficients of the order $\kappa_{\rm CR} \propto 10^{28}$–$10^{29}$ cm s^{-1} (e.g., Strong & Moskalenko 1998, Trotta et al. 2011, Tabatabaei et al. 2013). Locally the diffusion might be anisotropic with significantly smaller coefficients perpendicular to the magnetic field lines. On global galactic scales of the Milky Way, however, the diffusion can be considered isotropic (Strong et al. 2007). The lifetime of the several gigaelectronvolt CR fluid is known from radioactive dating to be roughly 10 million years.

In addition to thermal and radiation pressure caused by stellar feedback, CRs turn out to be an important agent on galactic scales and, once accelerated in regions of local feedback from star formation, they might be efficient in supporting or even driving galactic outflows. At the beginning of the 1990s it was proposed that the combined effect of thermal pressure, magnetohydrodynamic (MHD) waves, and an effective (nonthermal) CR pressure (McKenzie & Voelk 1982) is able to drive a galactic wind (Breitschwerdt et al. 1991, 1993), even if the star-formation rate is moderate. Recent observations of the starburst galaxy M82 (VERITAS Collaboration et al. 2009) reveal CR densities that are 500 times higher than those in the Milky Way and thus clearly link the CR density with regions of highly efficient star formation. Other groups have argued that the galactic wind in M82 is purely driven by strong stellar feedback (Chevalier & Clegg 1985, Völk et al. 1996). However, in normal spirals like the Milky Way, stellar feedback is probably not strong enough to drive a large-scale galactic wind. Nevertheless, recent ROSAT observations of the Milky Way show extended, soft X-ray emission, which is best explained with a kiloparsec-scale wind for which the CR pressure may be essential (Everett et al. 2008).

In galaxy-scale hydrodynamics simulations with SPH and AMR codes, CRs have recently been included as a separate fluid, as their mean free path is shorter than the typical length scales resolved (Skilling 1975). The fluid is treated as a relativistic gas with $\gamma_{\rm cr} = 4/3$ and is advected with the gas. The resulting total pressure is $p_{\rm tot} = p_{\rm th} + p_{\rm cr}$ with $p_{\rm cr} = (\gamma_{\rm cr} - 1)E_{\rm cr}$. In addition the CRs are allowed to diffuse through the ISM. This is treated approximately by either streaming (Uhlig et al. 2012) or isotropic diffusion with a typical diffusion coefficient (Enßlin et al. 2007, Jubelgas et al. 2008, Booth et al. 2013, Salem & Bryan 2014). In simulations following magnetic fields the diffusion is treated anisotropically with one or two orders of magnitude lower diffusion coefficients along the magnetic field lines (Yang et al. 2012, Hanasz et al. 2013, Pakmor et al. 2016).

All simulations that include CRs on galactic scales indicate that they can significantly support the driving of bipolar galactic winds with velocities exceeding the local escape speed and with mass-loading greater than unity. The winds are driven by the additional pressure gradient due to CRs in low-density regions (Uhlig et al. 2012, Booth et al. 2013, Hanasz et al. 2013, Salem & Bryan 2014, Pakmor et al. 2016, Salem et al. 2016). This process is only efficient if CRs can diffuse out of the high-density regions, where they are dynamically unimportant, to build up a galaxywide vertical gradient (see, e.g., Uhlig et al. 2012, Booth et al. 2013). The mass-loading of CR-driven winds is higher for lower-mass galaxies (Wadepuhl & Springel 2011, Uhlig et al. 2012, Booth et al. 2013), but also for gas-rich massive galaxies the effect is significant (Hanasz et al. 2013). CR-driven outflows can also support stable configurations of open magnetic field lines originating from regions of high star-formation rates (Hanasz et al. 2013). These simulations might also be able to explain the detection of strong magnetic fields at large radii ($\sim$50 kpc) around star-forming galaxies at intermediate and high redshift (Bernet et al. 2013).

Recently, simulations of the impact of CRs on the ISM on smaller scales have confirmed the ideas brought forward by larger-scale galaxy formation simulations and analytic estimates. It was shown by Girichidis et al. (2016a), using MHD simulations with anisotropic diffusion, that CRs indeed support the launching of outflows from galactic disks and the basic results seem to be insensitive of the MHD method used, the details of the star formation algorithm, and the presence of self-gravity (Simpson et al. 2016). It remains to be seen whether the supporting role of CRs (i.e., the pressure gradient) for the driving of outflows is significant or whether the computations still suffer from inaccuracies in capturing the accurate effect of supernova explosions on the formation of a hot, wind-driving, gas phase.

The simulations presented above can only be the starting point for more detailed investigations of the potential importance of CRs for the driving of galactic outflows. In galaxy-scale simulations, the galactic ISM is in general unresolved, with a significantly simplified treatment of energy injection by supernovae as well as CR transport. Also the global and local evolution of the galactic magnetic field has to be considered and significant progress has been made recently (Dolag et al. 2005, 2008; Dolag & Stasyszyn 2009, Kotarba et al. 2009, 2010; Dubois & Teyssier 2010; Pakmor & Springel 2013; Pakmor et al. 2014, 2016; Rieder & Teyssier 2016). If it turns out that CRs and magnetic fields are indeed as important as suggested, they have the potential to be global players, regulating the evolution of the ISM and the efficiency of galaxy formation across cosmic times.

3.5. Mechanical and Radiative AGN Feedback

Although the significant work done by many groups using thermal AGN feedback (see Section 2.3) has solid motivation and has produced many quite useful results, the somewhat arbitrary physical implementation has troubling aspects that several groups have attempted to remedy. First, there is no physical means specified for communicating the energy from the black holes to the surrounding gas in these treatments [see discussion by Ostriker et al. (2010)]. In actual AGN systems there are high-velocity winds and radiation output, both of which require consideration of momentum associated with the energy transfer and a spatial direction for the momentum outflow (Churazov et al. 2005, Merloni & Heinz 2008, Fabian 2012). But in a purely thermal feedback approach these physical factors are missing and, more importantly, the mass to which the thermal feedback energy is distributed is not specified or defined by a heating threshold (Section 2.3). Adding this energy to a very small mass would produce very high temperatures and radiative energy losses, and adding it to a very large mass would produce small additional velocities compared to the virial velocities in the galaxy; so adding it to the just-right amount of mass seems to be required.

But if the added feedback energy is deposited with the appropriate accompanying momentum, as observed in broad absorption line winds, the energy redistribution is achieved by physical means.

There exists a characteristic electromagnetic spectrum for AGNs with peaks in the IR, UV, and X-ray bands (e.g., Sazonov et al. 2004) that can be taken as the emitted output with the ratio of electromagnetic output to mass accretion given by the Soltan argument (Soltan 1982). In addition to relativistic jets there are also broadline winds observed to be commonly emitted by AGNs (Yuan & Narayan 2014), and these too have been calibrated to the accretion rate empirically (Arav et al. 2013; see also Krolik 1999). Thus one can specify the output in mass, energy, momentum, and radiation in various bands per mass accreted on the basis of approximate matches to observed AGNs, and then the thermal, mechanical and radiative coupling of these components to the surrounding medium should be handled automatically by the hydro codes being utilized. When taking this approach (and including the Eddington force rather than putting in a limit) the accretion rate self-adjusts, so no arbitrary multiplicative boost factors are needed in implementing the Bondi–Lyttleton accretion. First attempts to approximately include the effects of UV and X-ray emission from accreting black holes have been made (e.g., Hambrick et al. 2011, Vogelsberger et al. 2013, Choi et al. 2015, Roos et al. 2015, Bieri et al. 2017). Both mechanical (broad absorption line) and radiative effects are included in Choi et al. (2016) for cosmological simulations and in Hopkins et al. (2016) for high-resolution simulations of galactic centers. However, in the end, the results of this more complex approach are in fact similar to those of the thermal feedback approach with regard to regulating the overall mass growth of the central black hole, but other aspects are very different. For example, the fluctuation level of the kinetic feedback is far more extreme, with on periods rarely exceeding several million years and a small overall duty cycle being expected. And, as noted earlier, correct prediction of the thermal X-ray emission from massive galaxies provides a strong test of the feedback mechanism that indicates that including a kinetic wind component is essential (Choi et al. 2015, Weinberger et al. 2017).

Jets from AGNs are frequently observed and feedback from this mechanism is sometimes called radio mode (Fabian 2012, Heckman & Best 2014). Some cosmological galaxy evolution treatments have included this process (e.g., Dubois et al. 2014), the reality of which is not in doubt. But narrow relativistic jets effectively drill through the ISM within galaxies, leaving a dramatic imprint on the surrounding cluster gas but probably not communicating significant amounts of energy or momentum to the ISM of the parent galaxy (Vernaleo & Reynolds 2006). However, potential coupling mechanisms, e.g., turbulent mixing and dissipation, exist and are studied in detail with higher-resolution simulations (Omma et al. 2004, Scannapieco & Brüggen 2008, Gaspari et al. 2012, Babul et al. 2013, Li & Bryan 2014). Jets being extremely important in regulating cooling flows within clusters is probably less important than other, more prosaic processes in determining the internal evolution of galaxies.

4. CONCLUSION & OUTLOOK

Since the advent of self-consistent cosmological numerical simulations about 35 years ago significant progress in understanding galaxy formation has been made. Modern supercomputers and numerical algorithms have become powerful enough to allow the simulation of individual galaxies at relatively high resolution as well as the evolution of galaxy populations in representative cosmological volumes. With different numerical techniques (SPH, meshless particle hydrodynamics, AMR, and moving-mesh hydrodynamics; see review by Somerville & Davé 2015) it is now possible to simulate galaxy populations (at spatial resolutions of 0.5–3 kpc) with a realistic cosmological evolution of sizes, abundances, star-formation rates, dark matter fractions, and gas fractions as well as stellar and black hole masses from well-defined initial conditions, for a direct comparison

with observational galaxy surveys (e.g., Davé et al. 2013, Hirschmann et al. 2014, Khandai et al. 2015, Schaye et al. 2015, Sijacki et al. 2015).

Zoom simulations of individual galaxies (at resolutions <500 pc) allow detailed investigation of the formation processes and the consequences for the internal galaxy structure for direct comparison to high-resolution observations (e.g., Guedes et al. 2011, Dubois et al. 2013, Stinson et al. 2013, Aumer et al. 2014, Genel et al. 2014, Hopkins et al. 2014, Marinacci et al. 2014a, Naab et al. 2014, Wetzel et al. 2016). Simulations of this kind (see also Renaud et al. 2015, Rosdahl et al. 2015, Forbes et al. 2016, Hu et al. 2016, Richings & Schaye 2016) with high enough spatial resolution to represent the multiphase ISM structure and stellar feedback and more accurately account for major effects like stellar winds, radiation, and supernovae have the potential to shed more light into the detailed physical processes governing galaxy formation.

The rapid recent progress can be considered a success in our quest for a better understanding of galaxy formation. It was mainly triggered by the perception that thermal energy input from supernovae is most likely insufficient to trigger outflows and galactic winds, and now other mechanisms are being explored as the relevant drivers. These outflows, however, play a major—if not the dominant—role for regulating the formation of galaxies at low and high masses. They are most likely driven by energy injection from newly formed stellar populations (CRs, radiation and winds, in addition to supernovae) and accreting black holes. As the outflows are launched on parsec and subparsec scales, well below the resolution and physical complexity limit of any cosmological simulation, this has triggered a wealth of subresolution models for stellar and AGN feedback (see Sections 2.2.1 and 2.3). The fact that many models—even if conceptually very different—driving a reasonable galactic wind can successfully reproduce galaxy abundances and disk galaxy morphologies (see, e.g., **Figures 4** and **2**) indicates that the essential characteristics of the problem have been disclosed. However, the empirical nature of the subresolution models limits the predictive power of the simulations, and the literature becomes enriched by parameter studies of particular implementations despite obvious shortcomings of the respective models that are compensated by adjusted parameters. Delayed cooling, stochastic thermal, and nonthermal feedback models may significantly overestimate the energy and momentum input into the ISM, and the delay timescales are uncertain. Decoupled wind models might not capture (i.e., underestimate) the energy coupling to the local ISM and result in unrealistic wind structures. Empirical momentum-driving models rely on uncertain coupling efficiencies for IR radiation. Similarly, almost all AGN feedback models—on cosmological scales—are of empirical nature with accretion and energy conversion efficiencies adjusted, in a plausible fashion, to match observed scaling relations.

It will be a major challenge in theoretical galaxy formation to understand stellar and AGN feedback in detail and identify physically correct subresolution models taking into account all relevant physical processes. First promising steps in this direction have been made from high-resolution galaxy-scale simulations as well as simulations on smaller scales. A full accounting for the energy input from stellar populations (e.g., Hopkins et al. 2012b, Agertz et al. 2013), the long-range effect of low- and high-energy radiation from stars and AGNs (e.g., Choi et al. 2012, Vogelsberger et al. 2013, Kannan et al. 2014, Roos et al. 2015, Rosdahl et al. 2015, Bieri et al. 2017), and the consideration of other significant nonthermal components of the ISM, namely magnetic fields and CRs (e.g., Uhlig et al. 2012, Booth et al. 2013, Hanasz et al. 2013, Salem & Bryan 2014, Pakmor et al. 2016), are probably the most promising areas of galaxy-formation research in the future. These research directions mainly refer to problem B of our physics problem (Section 1.1): the knowledge of the physical processes primarily responsible for understanding each phase of galactic evolution. Starting with well-defined initial conditions, we can now roughly reproduce the scales and internal structures of common galaxy types and labor with increasing physical precision

to correctly model the detailed processes involved in feedback from stars and supermassive black holes.

DISCLOSURE STATEMENT

The authors are not aware of any affiliations, memberships, funding, or financial holdings that might be perceived as affecting the objectivity of this review.

ACKNOWLEDGMENTS

The authors acknowledge valuable input on the manuscript from O. Agertz, R. Davé, A. Dekel, Y. Dubois, P. Girichidis, M. Hanasz, M. Hirschmann, P. Hopkins, N. Khandai, B. Moster, T. Peters, E. Puchwein, M. Rafieferantsoa, V. Springel, G. Stinson, R. Teyssier, H. Übler, M. Vogelsberger, and S. Zhukovska. The authors are particularly grateful for the many detailed and valuable comments from J. Kormendy, D. Nelson, and J. Schaye.

LITERATURE CITED

Abadi MG, Navarro JF, Steinmetz M, Eke VR. 2003a. *Ap. J.* 591:499–514
Abadi MG, Navarro JF, Steinmetz M, Eke VR. 2003b. *Ap. J.* 597:21–34
Ackermann M, Ajello M, Allafort A, et al. 2013. *Science* 339:807–11
Agertz O, Kravtsov AV. 2015. *Ap. J.* 804:18
Agertz O, Kravtsov AV, Leitner SN, Gnedin NY. 2013. *Ap. J.* 770:25
Agertz O, Moore B, Stadel J, et al. 2007. *MNRAS* 380:963–78
Agertz O, Teyssier R, Moore B. 2011. *MNRAS* 410:1391–408
Anderson ME, Gaspari M, White SDM, Wang W, Dai X. 2015. *MNRAS* 449:3806–26
Anglés-Alcázar D, Davé R, Faucher-Giguère CA, Özel F, Hopkins PF. 2017. *MNRAS* 464:2840–53
Anglés-Alcázar D, Davé R, Özel F, Oppenheimer BD. 2014. *Ap. J.* 782:84
Anglés-Alcázar D, Özel F, Davé R. 2013. *Ap. J.* 770:5
Angulo RE, Springel V, White SDM, et al. 2012. *MNRAS* 426:2046–62
Arav N, Borguet B, Chamberlain C, Edmonds D, Danforth C. 2013. *MNRAS* 436:3286–305
Arthur SJ, Kurtz SE, Franco J, Albarrán MY. 2004. *Ap. J.* 608:282–96
Aumer M, White SDM, Naab T. 2014. *MNRAS* 441:3679–95
Aumer M, White SDM, Naab T, Scannapieco C. 2013. *MNRAS* 434:3142–64
Babul A, Sharma P, Reynolds CS. 2013. *Ap. J.* 768:11
Bahé YM, Crain RA, Kauffmann G, et al. 2016. *MNRAS* 456:1115–36
Balogh ML, Pearce FR, Bower RG, Kay ST. 2001. *MNRAS* 326:1228–34
Barai P, Viel M, Borgani S, et al. 2013. *MNRAS* 430:3213–34
Barai P, Viel M, Murante G, Gaspari M, Borgani S. 2014. *MNRAS* 437:1456–75
Barnes JE. 1988. *Ap. J.* 331:699–717
Barnes JE. 1992. *Ap. J.* 393:484–507
Barnes JE. 1998. In *Galaxies: Interactions and Induced Star Formation, Saas-Fee Advanced Course 26. Lecture Notes 1996.* Swiss Soc. Astrophys. Astron. XIV. Berlin/Heidelburg: Springer-Verlag
Barnes JE. 2002. *MNRAS* 333:481–94
Barnes JE, Hernquist L. 1992. *Annu. Rev. Astron. Astrophys.* 30:705–42
Barnes JE, Hernquist L. 1996. *Ap. J.* 471:115
Bédorf J, Portegies Zwart S. 2013. *MNRAS* 431:767–80
Behroozi PS, Conroy C, Wechsler RH. 2010. *Ap. J.* 717:379–403
Behroozi PS, Wechsler RH, Conroy C. 2013. *Ap. J.* 770:57
Bekki K. 1998. *Ap. J. Lett.* 502:L133
Bekki K. 2015. *MNRAS* 449:1625–49

Bekki K, Shioya Y. 1997. *Ap. J. Lett.* 478:L17
Bell AR. 1978. *MNRAS* 182:147–56
Bendo GJ, Barnes JE. 2000. *MNRAS* 316:315–25
Berlind AA, Weinberg DH. 2002. *Ap. J.* 575:587–616
Bernardi M, Meert A, Sheth RK, et al. 2013. *MNRAS* 436:697–704
Bernet ML, Miniati F, Lilly SJ. 2013. *Ap. J. Lett.* 772:L28
Bezanson R, van Dokkum PG, Tal T, et al. 2009. *Ap. J.* 697:1290–98
Bieri R, Dubois Y, Rosdahl J, et al. 2017. *MNRAS* 464:1854–73
Bigiel F, Leroy A, Walter F, et al. 2008. *Astron. J.* 136:2846–71
Binney J. 1977. *Ap. J.* 215:483–91
Binney J, Tabor G. 1995. *MNRAS* 276:663
Binney J, Tremaine S. 2008. *Galactic Dynamics: Second Edition*. Princeton, NJ: Princeton Univ. Press
Birnboim Y, Dekel A. 2003. *MNRAS* 345:349–64
Blaauw A. 1961. *Bull. Astron. Inst. Neth.* 15:265
Bland-Hawthorn J, Gerhard O. 2016. *Annu. Rev. Astron. Astrophys.* 54:529–96
Blandford RD, Ostriker JP. 1978. *Ap. J. Lett.* 221:L29–32
Blanton MR, Moustakas J. 2009. *Annu. Rev. Astron. Astrophys.* 47:159–210
Blondin JM, Wright EB, Borkowski KJ, Reynolds SP. 1998. *Ap. J.* 500:342–54
Bluck AFL, Conselice CJ, Bouwens RJ, et al. 2009. *MNRAS* 394:L51–55
Bogdán Á, Forman WR, Vogelsberger M, et al. 2013. *Ap. J.* 772:97
Bois M, Bournaud F, Emsellem E, et al. 2010. *MNRAS* 406:2405–20
Bois M, Emsellem E, Bournaud F, et al. 2011. *MNRAS* 416:1654–79
Bondi H. 1952. *MNRAS* 112:195
Bondi H, Hoyle F. 1944. *MNRAS* 104:273
Booth CM, Agertz O, Kravtsov AV, Gnedin NY. 2013. *Ap. J. Lett.* 777:L16
Booth CM, Schaye J. 2009. *MNRAS* 398:53–74
Boulares A, Cox DP. 1990. *Ap. J.* 365:544–58
Bournaud F, Chapon D, Teyssier R, et al. 2011a. *Ap. J.* 730:4
Bournaud F, Combes F, Jog CJ. 2004. *Astron. Astrophys.* 418:L27–L30
Bournaud F, Dekel A, Teyssier R, et al. 2011b. *Ap. J. Lett.* 741:L33
Bournaud F, Jog CJ, Combes F. 2005. *Astron. Astrophys.* 437:69–85
Bournaud F, Jog CJ, Combes F. 2007. *Astron. Astrophys.* 476:1179–90
Bouwens RJ, Illingworth GD, Oesch PA, et al. 2012. *Ap. J.* 754:83
Bovy J, Allende Prieto C, Beers TC, et al. 2012. *Ap. J.* 759:131
Bower RG, Benson AJ, Malbon R, et al. 2006. *MNRAS* 370:645–55
Boylan-Kolchin M, Bullock JS, Kaplinghat M. 2011. *MNRAS* 415:L40–44
Boylan-Kolchin M, Ma CP, Quataert E. 2005. *MNRAS* 362:184–96
Breitschwerdt D, McKenzie JF, Voelk HJ. 1991. *Astron. Astrophys.* 245:79–98
Breitschwerdt D, McKenzie JF, Voelk HJ. 1993. *Astron. Astrophys.* 269:54–66
Brighenti F, Mathews WG. 2006. *Ap. J.* 643:120–27
Brook CB, Governato F, Roskar R, et al. 2011. *MNRAS* 415:1051–60
Brook CB, Stinson G, Gibson BK, et al. 2012. *MNRAS* 419:771–79
Brook CB, Stinson G, Gibson BK, et al. 2014. *MNRAS* 443:3809–18
Bryan GL, Norman ML, O'Shea BW, et al. 2014. *Ap. J. Suppl.* 211:19
Bryan SE, Mao S, Kay ST, et al. 2012. *MNRAS* 422:1863–79
Bullock JS, Wechsler RH, Somerville RS. 2002. *MNRAS* 329:246–56
Bundy K, Bershady MA, Law DR, et al. 2015. *Ap. J.* 798:7
Cappellari M, Emsellem E, Krajnović D, et al. 2011a. *MNRAS* 416:1680–96
Cappellari M, Emsellem E, Krajnović D, et al. 2011b. *MNRAS* 413:813–36
Caprioli D, Pop AR, Spitkovsky A. 2015. *Ap. J. Lett.* 798:L28
Castor JI, Abbott DC, Klein RI. 1975. *Ap. J.* 195:157–74
Catinella B, Schiminovich D, Kauffmann G, et al. 2010. *MNRAS* 403:683–708
Cen R, Ostriker JP. 1992a. *Ap. J.* 393:22–41

Cen R, Ostriker JP. 1992b. *Ap. J. Lett.* 399:L113–16
Cenarro AJ, Trujillo I. 2009. *Ap. J. Lett.* 696:L43–47
Ceverino D, Klypin A. 2009. *Ap. J.* 695:292–309
Chevalier RA. 1982. *Ap. J.* 258:790–97
Chevalier RA, Clegg AW. 1985. *Nature* 317:44
Choi E, Naab T, Ostriker JP, Johansson PH, Moster BP. 2014. *MNRAS* 442:440–53
Choi E, Ostriker JP, Naab T, Johansson PH. 2012. *Ap. J.* 754:125
Choi E, Ostriker JP, Naab T, Oser L, Moster BP. 2015. *MNRAS* 449:4105–16
Choi E, Ostriker JP, Naab T, et al. 2016. *Ap. J.* Accepted. arXiv:1610.09389
Christensen C, Quinn T, Governato F, et al. 2012. *MNRAS* 425:3058–76
Christensen CR, Davé R, Governato F, et al. 2016. *Ap. J.* 824:57
Churazov E, Sazonov S, Sunyaev R, et al. 2005. *MNRAS* 363:L91–95
Cimatti A, Nipoti C, Cassata P. 2012. *MNRAS* 422:L62
Cioffi DF, McKee CF, Bertschinger E. 1988. *Ap. J.* 334:252–65
Ciotti L, D'Ercole A, Pellegrini S, Renzini A. 1991. *Ap. J.* 376:380–403
Ciotti L, Ostriker JP. 1997. *Ap. J. Lett.* 487:L105–8
Ciotti L, Ostriker JP. 2001. *Ap. J.* 551:131–52
Cisternas M, Jahnke K, Inskip KJ, et al. 2011. *Ap. J.* 726:57
Cole S, Lacey CG, Baugh CM, Frenk CS. 2000. *MNRAS* 319:168–204
Conroy C, Wechsler RH. 2009. *Ap. J.* 696:620–35
Conroy C, Wechsler RH, Kravtsov AV. 2006. *Ap. J.* 647:201–14
Courteau S, Cappellari M, de Jong RS, et al. 2014. *Rev. Mod. Phys.* 86:47–119
Cox TJ, Dutta SN, Di Matteo T, et al. 2006a. *Ap. J.* 650:791–811
Cox TJ, Jonsson P, Primack JR, Somerville RS. 2006b. *MNRAS* 373:1013–38
Crain RA, McCarthy IG, Frenk CS, Theuns T, Schaye J. 2010. *MNRAS* 407:1403–22
Crain RA, Schaye J, Bower RG, et al. 2015. *MNRAS* 450:1937–61
Cretton N, Naab T, Rix HW, Burkert A. 2001. *Ap. J.* 554:291–97
Croton DJ, Springel V, White SDM, et al. 2006. *MNRAS* 365:11–28
D'Onghia E, Burkert A. 2004. *Ap. J. Lett.* 612:L13–16
Daddi E, Bournaud F, Walter F, et al. 2010. *Ap. J.* 713:686–707
Daddi E, Dickinson M, Morrison G, et al. 2007. *Ap. J.* 670:156–72
Daddi E, Renzini A, Pirzkal N, et al. 2005. *Ap. J.* 626:680–97
Dai X, Bregman JN, Kochanek CS, Rasia E. 2010. *Ap. J.* 719:119–25
Dalcanton JJ, Spergel DN, Summers FJ. 1997. *Ap. J.* 482:659–76
Dale JE, Bonnell IA. 2008. *MNRAS* 391:2–13
Dale JE, Bonnell IA, Whitworth AP. 2007. *MNRAS* 375:1291–98
Dale JE, Ngoumou J, Ercolano B, Bonnell IA. 2013. *MNRAS* 436:3430–45
Dale JE, Ngoumou J, Ercolano B, Bonnell IA. 2014. *MNRAS* 442:694–712
Dalla Vecchia C, Schaye J. 2008. *MNRAS* 387:1431–44
Dalla Vecchia C, Schaye J. 2012. *MNRAS* 426:140–58
Damjanov I, Abraham RG, Glazebrook K, et al. 2011. *Ap. J. Lett.* 739:L44
Davé R, Finlator K, Oppenheimer BD. 2011. *MNRAS* 416:1354–76
Davé R, Katz N, Oppenheimer BD, Kollmeier JA, Weinberg DH. 2013. *MNRAS* 434:2645–63
Davé R, Thompson RJ, Hopkins PF. 2016. *MNRAS* 462:3265–84
Davis SW, Jiang YF, Stone JM, Murray N. 2014. *Ap. J.* 796:107
de Avillez MA. 2000. *MNRAS* 315:479–97
de Avillez MA, Breitschwerdt D. 2004. *Astron. Astrophys.* 425:899–911
de Avillez MA, Breitschwerdt D. 2005. *Astron. Astrophys.* 436:585–600
De Lucia G, Blaizot J. 2007. *MNRAS* 375:2–14
de Vaucouleurs G. 1948. *Ann. Astrophys.* 11:247
de Zeeuw PT, Bureau M, Emsellem E, et al. 2002. *MNRAS* 329:513–30
Debuhr J, Quataert E, Ma CP. 2011. *MNRAS* 412:1341–60
Debuhr J, Quataert E, Ma CP, Hopkins P. 2010. *MNRAS* 406:L55–59

Dekel A, Birnboim Y, Engel G, et al. 2009. *Nature* 457:451–54
Dekel A, Cox TJ. 2006. *MNRAS* 370:1445–53
Dekel A, Silk J. 1986. *Ap. J.* 303:39–55
Di Matteo P, Jog CJ, Lehnert MD, Combes F, Semelin B. 2009a. *Astron. Astrophys.* 501:L9–13
Di Matteo P, Pipino A, Lehnert MD, Combes F, Semelin B. 2009b. *Astron. Astrophys.* 499:427–37
Di Matteo T, Khandai N, DeGraf C, et al. 2012. *Ap. J. Lett.* 745:L29
Di Matteo T, Springel V, Hernquist L. 2005. *Nature* 433:604–7
Diemand J, Kuhlen M, Madau P. 2007. *Ap. J.* 667:859–77
Dolag K, Bykov AM, Diaferio A. 2008. *Space Sci. Rev.* 134:311–35
Dolag K, Grasso D, Springel V, Tkachev I. 2005. *J. Cosmol. Astropart. Phys.* 1:9
Dolag K, Stasyszyn F. 2009. *MNRAS* 398:1678–97
Draine BT. 2011. *Physics of the Interstellar and Intergalactic Medium*. Princeton, NJ: Princeton Univ. Press
Dressler A. 1980. *Ap. J.* 236:351–65
Dubois Y, Devriendt J, Slyz A, Teyssier R. 2012. *MNRAS* 420:2662–83
Dubois Y, Gavazzi R, Peirani S, Silk J. 2013. *MNRAS* 433:3297–313
Dubois Y, Pichon C, Welker C, et al. 2014. *MNRAS* 444:1453–68
Dubois Y, Teyssier R. 2010. *Astron. Astrophys.* 523:A72
Duncan K, Conselice CJ, Mortlock A, et al. 2014. *MNRAS* 444:2960–84
Efstathiou G, Eastwood JW. 1981. *MNRAS* 194:503–25
Eggen OJ, Lynden-Bell D, Sandage AR. 1962. *Ap. J.* 136:748
Ellison DC, Patnaude DJ, Slane P, Raymond J. 2010. *Ap. J.* 712:287–93
Elmegreen BG, Scalo J. 2004. *Annu. Rev. Astron. Astrophys.* 42:211–73
Enßlin TA, Pfrommer C, Springel V, Jubelgas M. 2007. *Astron. Astrophys.* 473:41–57
Everett JE, Zweibel EG, Benjamin RA, et al. 2008. *Ap. J.* 674:258–70
Evrard AE. 1988. *MNRAS* 235:911–34
Fabian AC. 2012. *Annu. Rev. Astron. Astrophys.* 50:455–89
Fabian AC, Sanders JS, Taylor GB, et al. 2006. *MNRAS* 366:417–28
Fabjan D, Borgani S, Tornatore L, et al. 2010. *MNRAS* 401:1670–90
Fagioli M, Carollo CM, Renzini A, et al. 2016. *Ap. J.* 831:173
Fall SM. 1979. *Nature* 281:200–2
Fall SM, Efstathiou G. 1980. *MNRAS* 193:189–206
Farouki RT, Shapiro SL. 1982. *Ap. J.* 259:103–15
Faucher-Giguère CA, Lidz A, Zaldarriaga M, Hernquist L. 2009. *Ap. J.* 703:1416–43
Feldmann R, Carollo CM, Mayer L. 2011. *Ap. J.* 736:88
Feldmann R, Carollo CM, Mayer L, et al. 2010. *Ap. J.* 709:218–40
Feldmann R, Gnedin NY, Kravtsov AV. 2012. *Ap. J.* 747:124
Feldmann R, Mayer L. 2015. *MNRAS* 446:1939–56
Ferrière KM. 2001. *Rev. Mod. Phys.* 73:1031–66
Finlator K, Davé R. 2008. *MNRAS* 385:2181–204
Fogarty LMR, Scott N, Owers MS, et al. 2014. *MNRAS* 443:485–503
Forbes JC, Krumholz MR, Goldbaum NJ, Dekel A. 2016. *Nature* 535:523–25
Förster Schreiber NM, Genzel R, Bouché N, et al. 2009. *Ap. J.* 706:1364–428
Frenk CS, White SDM. 2012. *Ann. Phys.* 524:507–34
Frenk CS, White SDM, Bode P, et al. 1999. *Ap. J.* 525:554–82
Fryxell B, Olson K, Ricker P, et al. 2000. *Ap. J. Suppl.* 131:273–334
Furlong M, Bower RG, Theuns T, et al. 2015. *MNRAS* 450:4486–504
Gabor JM, Bournaud F. 2013. *MNRAS* 434:606–20
Gabor JM, Davé R. 2012. *MNRAS* 427:1816–29
Gaburov E, Nitadori K. 2011. *MNRAS* 414:129–54
Gao L, Navarro JF, Frenk CS, et al. 2012. *MNRAS* 425:2169–86
Gaspari M, Brighenti F, Temi P. 2012. *MNRAS* 424:190–209
Gatto A, Walch S, Mac Low MM, et al. 2015. *MNRAS* 449:1057–75
Gatto A, Walch S, Naab T, et al. 2017. *MNRAS* 466:1903–24

Geen S, Hennebelle P, Tremblin P, Rosdahl J. 2016. *MNRAS* 463:3129–42
Geen S, Rosdahl J, Blaizot J, Devriendt J, Slyz A. 2015. *MNRAS* 448:3248–64
Genel S, Fall SM, Hernquist L, et al. 2015. *Ap. J. Lett.* 804:L40
Genel S, Naab T, Genzel R, et al. 2012. *Ap. J.* 745:11
Genel S, Vogelsberger M, Nelson D, et al. 2013. *MNRAS* 435:1426–42
Genel S, Vogelsberger M, Springel V, et al. 2014. *MNRAS* 445:175–200
Genzel R, Eckart A, Ott T, Eisenhauer F. 1997. *MNRAS* 291:219–34
Genzel R, Förster Schreiber NM, Rosario D, et al. 2014. *Ap. J.* 796:7
Genzel R, Tacconi LJ, Eisenhauer F, et al. 2006. *Nature* 442:786–89
Georgakakis A, Coil AL, Laird ES, et al. 2009. *MNRAS* 397:623–33
Gerritsen JPE. 1997. *Star formation and the interstellar medium in galaxy simulations*. Ph.D. Thesis, Groningen University, The Netherlands
Gies DR, Bolton CT. 1986. *Ap. J. Suppl.* 61:419–54
Gingold RA, Monaghan JJ. 1977. *MNRAS* 181:375–89
Giodini S, Pierini D, Finoguenov A, et al. 2009. *Ap. J.* 703:982–93
Girichidis P, Naab T, Walch S, et al. 2016a. *Ap. J. Lett.* 816:L19
Girichidis P, Walch S, Naab T, et al. 2016b. *MNRAS* 456:3432–55
Glover SCO, Clark PC. 2012. *MNRAS* 421:9–19
Glover SCO, Mac Low MM. 2007. *Ap. J.* 659:1317–37
Gnat O, Sternberg A. 2007. *Ap. J. Suppl.* 168:213–30
Gnedin NY, Tassis K, Kravtsov AV. 2009. *Ap. J.* 697:55–67
Gonzalez AH, Sivanandam S, Zabludoff AI, Zaritsky D. 2013. *Ap. J.* 778:14
González-García AC, Balcells M. 2005. *MNRAS* 357:753–72
Governato F, Brook C, Mayer L, et al. 2010. *Nature* 463:203–6
Governato F, Mayer L, Wadsley J, et al. 2004. *Ap. J.* 607:688–96
Governato F, Willman B, Mayer L, et al. 2007. *MNRAS* 374:1479–94
Grand RJJ, Springel V, Gómez FA, et al. 2016. *MNRAS* 459:199–219
Gritschneder M, Burkert A, Naab T, Walch S. 2010. *Ap. J.* 723:971–84
Gritschneder M, Naab T, Walch S, Burkert A, Heitsch F. 2009. *Ap. J. Lett.* 694:L26–30
Guedes J, Callegari S, Madau P, Mayer L. 2011. *Ap. J.* 742:76
Guo Q, White S. 2014. *MNRAS* 437:3228–35
Guo Q, White S, Boylan-Kolchin M, et al. 2011. *MNRAS* 413:101–31
Guo Q, White S, Li C, Boylan-Kolchin M. 2010. *MNRAS* 404:1111–20
Guo Q, White SDM. 2008. *MNRAS* 384:2–10
Haardt F, Madau P. 2012. *Ap. J.* 746:125
Haid S, Walch S, Naab T, et al. 2016. *MNRAS* 460:2962–78
Hambrick DC, Ostriker JP, Naab T, Johansson PH. 2011. *Ap. J.* 738:16
Hanasz M, Lesch H, Naab T, et al. 2013. *Ap. J. Lett.* 777:L38
Hayward CC, Torrey P, Springel V, et al. 2014. *MNRAS* 442:1992–2016
Hearin AP, Watson DF. 2013. *MNRAS* 435:1313–24
Heavens A, Panter B, Jimenez R, Dunlop J. 2004. *Nature* 428:625–27
Heckman TM. 2003. In *Starburst-Driven Galactic Winds*, ed. V Avila-Reese, C Firmani, CS Frenk, C Allen. *Rev. Mex. Astron. Astrofis. Conf. Ser.* 17:47. Mexico City, Mex.: Univ. Nac. Autón. Mex.
Heckman TM, Armus L, Miley GK. 1990. *Ap. J. Suppl.* 74:833–68
Heckman TM, Best PN. 2014. *Annu. Rev. Astron. Astrophys.* 52:589–660
Heckman TM, Lehnert MD, Strickland DK, Armus L. 2000. *Ap. J. Suppl.* 129:493–516
Heitsch F, Naab T, Walch S. 2011. *MNRAS* 415:271–78
Hennebelle P, Iffrig O. 2014. *Astron. Astrophys.* 570:A81
Henriques BMB, White SDM, Thomas PA, et al. 2015. *MNRAS* 451:2663–80
Hernquist L. 1989. *Nature* 340:687–91
Hernquist L. 1992. *Ap. J.* 400:460–75
Hernquist L. 1993a. *Ap. J.* 409:548–62
Hernquist L. 1993b. *Ap. J. Suppl.* 86:389–400

Hernquist L, Katz N. 1989. *Ap. J. Suppl.* 70:419–46
Hewitt JW, Yusef-Zadeh F, Wardle M. 2009. *Ap. J. Lett.* 706:L270–74
Heyl JS, Hernquist L, Spergel DN. 1994. *Ap. J.* 427:165–73
Hill AS, Joung MR, Mac Low MM, et al. 2012. *Ap. J.* 750:104
Hillas AM. 2005. *J. Phys. G Nucl. Phys.* 31:95
Hilz M, Naab T, Ostriker JP. 2013. *MNRAS* 429:2924–33
Hilz M, Naab T, Ostriker JP, et al. 2012. *MNRAS* 425:3119–36
Hirschmann M, Dolag K, Saro A, et al. 2014. *MNRAS* 442:2304–24
Hirschmann M, Naab T, Davé R, et al. 2013. *MNRAS* 436:2929–49
Hirschmann M, Naab T, Somerville RS, Burkert A, Oser L. 2012. *MNRAS* 419:3200–22
Hoffman L, Cox TJ, Dutta S, Hernquist L. 2009. *Ap. J.* 705:920–25
Hoffman L, Cox TJ, Dutta S, Hernquist L. 2010. *Ap. J.* 723:818–44
Hopkins PF. 2015. *MNRAS* 450:53–110
Hopkins PF, Cox TJ, Dutta SN, et al. 2009a. *Ap. J. Suppl.* 181:135–82
Hopkins PF, Hayward CC, Narayanan D, Hernquist L. 2012a. *MNRAS* 420:320–39
Hopkins PF, Hernquist L, Cox TJ, Keres D, Wuyts S. 2009b. *Ap. J.* 691:1424–58
Hopkins PF, Hernquist L, Cox TJ, et al. 2005. *Ap. J.* 630:705–15
Hopkins PF, Hernquist L, Cox TJ, et al. 2006. *Ap. J. Suppl.* 163:1–49
Hopkins PF, Kereš D, Murray N, et al. 2013a. *MNRAS* 433:78–97
Hopkins PF, Kereš D, Oñorbe J, et al. 2014. *MNRAS* 445:581–603
Hopkins PF, Lauer TR, Cox TJ, Hernquist L, Kormendy J. 2009c. *Ap. J. Suppl.* 181:486–532
Hopkins PF, Narayanan D, Murray N. 2013b. *MNRAS* 432:2647–53
Hopkins PF, Quataert E. 2011. *MNRAS* 415:1027–50
Hopkins PF, Quataert E, Murray N. 2011. *MNRAS* 417:950–73
Hopkins PF, Quataert E, Murray N. 2012b. *MNRAS* 421:3488–521
Hopkins PF, Quataert E, Murray N. 2012c. *MNRAS* 421:3522–37
Hopkins PF, Torrey P, Faucher-Giguère C-A, Quataert E, Murray N. 2016. *MNRAS* 458:816–31
Hoyle F, Lyttleton RA. 1939. *Proc. Camb. Philos. Soc.* 35:405–15
Hu CY, Naab T, Walch S, Glover SCO, Clark PC. 2016. *MNRAS* 458:3528–53
Hu CY, Naab T, Walch S, Moster BP, Oser L. 2014. *MNRAS* 443:1173–91
Hubber DA, Falle SAEG, Goodwin SP. 2013. *MNRAS* 432:711–27
Iffrig O, Hennebelle P. 2015. *Astron. Astrophys.* 576:A95
Janka HT. 2012. *Annu. Rev. Nucl. Part. Sci.* 62:407–51
Jesseit R, Cappellari M, Naab T, Emsellem E, Burkert A. 2009. *MNRAS* 397:1202–14
Jesseit R, Naab T. Peletier RF, Burkert A. 2007. *MNRAS* 376:997–1020
Johansson PH, Naab T, Burkert A. 2009a. *Ap. J.* 690:802–21
Johansson PH, Naab T, Ostriker JP. 2009b. *Ap. J. Lett.* 697:L38–43
Johansson PH, Naab T, Ostriker JP. 2012. *Ap. J.* 754:115
Joseph RD, Wright GS. 1985. *MNRAS* 214:87–95
Joung MKR, Mac Low MM. 2006. *Ap. J.* 653:1266–79
Jubelgas M, Springel V, Enßlin T, Pfrommer C. 2008. *Astron. Astrophys.* 481:33–63
Kalberla PMW, Kerp J. 2009. *Annu. Rev. Astron. Astrophys.* 47:27–61
Kang H, Jones TW. 2006. *Astropart. Phys.* 25:246–58
Kannan R, Stinson GS, Macciò AV, et al. 2014. *MNRAS* 437:2882–93
Katz N. 1992. *Ap. J.* 391:502–17
Katz N, Gunn JE. 1991. *Ap. J.* 377:365–81
Katz N, Weinberg DH, Hernquist L. 1996. *Ap. J. Suppl.* 105:19
Kauffmann G, Heckman TM, White SDM, et al. 2003. *MNRAS* 341:33–53
Kauffmann G, White SDM, Guiderdoni B. 1993. *MNRAS* 264:201
Keller BW, Wadsley J, Couchman HMP. 2015. *MNRAS* 453:3499–509
Keller BW, Wadsley J, Couchman HMP. 2016. *MNRAS* 463:1431–45
Kennicutt RC Jr. 1998. *Ap. J.* 498:541
Kennicutt RC Jr., Calzetti D, Walter F, et al. 2007. *Ap. J.* 671:333–48

Kennicutt RC Jr., Evans NJ. 2012. *Annu. Rev. Astron. Astrophys.* 50:531–608
Kereš D, Katz N, Weinberg DH, Davé R. 2005. *MNRAS* 363:2–28
Khandai N, Di Matteo T, Croft R, et al. 2015. *MNRAS* 450:1349–74
Khochfar S, Burkert A. 2006. *Astron. Astrophys.* 445:403–12
Khochfar S, Ostriker JP. 2008. *Ap. J.* 680:54–69
Khochfar S, Silk J. 2006. *MNRAS* 370:902–10
Kim CG, Kim WT, Ostriker EC. 2011. *Ap. J.* 743:25
Kim CG, Ostriker EC. 2015a. *Ap. J.* 802:99
Kim CG, Ostriker EC. 2015b. *Ap. J.* 815:67
Kim CG, Ostriker EC, Kim WT. 2013. *Ap. J.* 776:1
Kim J, Abel T, Agertz O, et al. 2014. *Ap. J. Suppl.* 210:14
Klypin AA, Trujillo-Gomez S, Primack J. 2011. *Ap. J.* 740:102
Kobayashi C. 2004. *MNRAS* 347:740–58
Kobayashi C. 2005. *MNRAS* 361:1216–26
Kocevski DD, Faber SM, Mozena M, et al. 2012. *Ap. J.* 744:148
Koopmans LVE, Bolton A, Treu T, et al. 2009. *Ap. J. Lett.* 703:L51–54
Kormendy J. 1999. In *Galaxy Dynamics: A Rutgers Symposium*, ed. DR Merritt, M Valluri, JA Sellwood. *ASP Conf. Ser.* 182:124–37. San Francisco: ASP
Kormendy J, Drory N, Bender R, Cornell ME. 2010. *Ap. J.* 723:54–80
Kormendy J, Fisher DB, Cornell ME, Bender R. 2009. *Ap. J. Suppl.* 182:216–309
Kormendy J, Freeman KC. 2016. *Ap. J.* 817:84
Kormendy J, Ho LC. 2013. *Annu. Rev. Astron. Astrophys.* 51:511–653
Korpi MJ, Brandenburg A, Shukurov A, Tuominen I, Nordlund Å. 1999. *Ap. J. Lett.* 514:L99–102
Kotarba H, Karl SJ, Naab T, et al. 2010. *Ap. J.* 716:1438–52
Kotarba H, Lesch H, Dolag K, et al. 2009. *MNRAS* 397:733–47
Kravtsov AV. 2003. *Ap. J. Lett.* 590:L1–4
Kravtsov AV, Berlind AA, Wechsler RH, et al. 2004. *Ap. J.* 609:35–49
Kravtsov AV, Borgani S. 2012. *Annu. Rev. Astron. Astrophys.* 50:353–409
Kravtsov AV, Klypin AA, Bullock JS, Primack JR. 1998. *Ap. J.* 502:48–58
Kravtsov AV, Klypin AA, Khokhlov AM. 1997. *Ap. J. Suppl.* 111:73–94
Kravtsov AV, Vikhlinin A, Meshscheryakov A. 2014. *Ap. J.* Submitted. arXiv:1401.7329
Krolik JH. 1999. *Active Galactic Nuclei: From the Central Black Hole to the Galactic Environment*. Princeton, NJ: Princeton Univ. Press
Krumholz MR. 2013. *MNRAS* 436:2747–62
Krumholz MR, Matzner CD. 2009. *Ap. J.* 703:1352–62
Krumholz MR, Matzner CD, McKee CF. 2006. *Ap. J.* 653:361–82
Krumholz MR, Thompson TA. 2012. *Ap. J.* 760:155
Krumholz MR, Thompson TA. 2013. *MNRAS* 434:2329–46
Kudritzki RP, Puls J. 2000. *Annu. Rev. Astron. Astrophys.* 38:613–66
Kuhlen M, Krumholz MR, Madau P, Smith BD, Wise J. 2012. *Ap. J.* 749:36
Kulsrud R, Pearce WP. 1969. *Ap. J.* 156:445
Lackner CN, Cen R, Ostriker JP, Joung MR. 2012. *MNRAS* 425:641–56
Laporte CFP, White SDM, Naab T, Gao L. 2013. *MNRAS* 435:901–9
Larson RB. 1974. *MNRAS* 169:229–46
Le Brun AMC, McCarthy IG, Melin JB. 2015. *MNRAS* 451:3868–81
Le Brun AMC, McCarthy IG, Schaye J, Ponman TJ. 2014. *MNRAS* 441:1270–90
Leitherer C, Schaerer D, Goldader JD, et al. 1999. *Ap. J. Suppl.* 123:3–40
Leroy AK, Walter F, Brinks E, et al. 2008. *Astron. J.* 136:2782–845
Li C, White SDM. 2009. *MNRAS* 398:2177–87
Li M, Bryan GL, Ostriker JP. 2017. *Ap. J.* 841:101
Li M, Ostriker JP, Cen R, Bryan GL, Naab T. 2015. *Ap. J.* 814:4
Li Y, Bryan GL. 2014. *Ap. J.* 789:54
Li Y, Mac Low MM, Klessen RS. 2005. *Ap. J. Lett.* 620:L19–22

Li YS, White SDM. 2008. *MNRAS* 384:1459–68
Lu Z, Mo HJ, Lu Y, et al. 2015. *MNRAS* 450:1604–17
Lucy LB. 1977. *Astron. J.* 82:1013–24
Mac Low MM, McCray R. 1988. *Ap. J.* 324:776–85
Malkov MA, O'C Drury L. 2001. *Rep. Prog. Phys.* 64:429–81
Man AWS, Toft S, Zirm AW, Wuyts S, van der Wel A. 2012. *Ap. J.* 744:85
Mandelbaum R, Seljak U, Kauffmann G, Hirata CM, Brinkmann J. 2006. *MNRAS* 368:715–31
Marinacci F, Fraternali F, Nipoti C, et al. 2011. *MNRAS* 415:1534–42
Marinacci F, Pakmor R, Springel V. 2014a. *MNRAS* 437:1750–75
Marinacci F, Pakmor R, Springel V, Simpson CM. 2014b. *MNRAS* 442:3745–60
Marri S, White SDM. 2003. *MNRAS* 345:561–74
Martin CL. 1999. *Ap. J.* 513:156–60
Martin CL. 2005. *Ap. J.* 621:227–45
Martin CL, Shapley AE, Coil AL, et al. 2013. *Ap. J.* 770:41
Martizzi D, Faucher-Giguère CA, Quataert E. 2015. *MNRAS* 450:504–22
Martizzi D, Fielding D, Faucher-Giguère CA, Quataert E. 2016. *MNRAS* 459:2311–26
Martizzi D, Jimmy, Teyssier R, Moore B. 2014. *MNRAS* 443:1500–8
Martizzi D, Teyssier R, Moore B. 2012a. *MNRAS* 420:2859–73
Martizzi D, Teyssier R, Moore B, Wentz T. 2012b. *MNRAS* 422:3081–91
Mathews WG. 1969. *Ap. J.* 157:583
McCarthy IG, Schaye J, Bower RG, et al. 2011. *MNRAS* 412:1965–84
McCarthy IG, Schaye J, Ponman TJ, et al. 2010. *MNRAS* 406:822–39
McKee CF, Ostriker JP. 1977. *Ap. J.* 218:148–69
McKenzie JF, Voelk HJ. 1982. *Astron. Astrophys.* 116:191–200
McKinnon R, Torrey P, Vogelsberger M. 2016. *MNRAS* 457:3775–800
Merloni A, Heinz S. 2008. *MNRAS* 388:1011–30
Meza A, Navarro JF, Steinmetz M, Eke VR. 2003. *Ap. J.* 590:619–35
Mihos JC, Hernquist L. 1994a. *Ap. J.* 437:611–24
Mihos JC, Hernquist L. 1994b. *Ap. J. Lett.* 431:L9–12
Mihos JC, Hernquist L. 1994c. *Ap. J. Lett.* 437:L47–50
Mihos JC, Hernquist L. 1996. *Ap. J.* 464:641–63
Mo H, van den Bosch FC, White S. 2010. *Galaxy Formation and Evolution.* Cambridge, UK: Cambridge Univ. Press
Mo HJ, Mao S, White SDM. 1998. *MNRAS* 295:319–36
Monaco P, Murante G, Borgani S, Dolag K. 2012. *MNRAS* 421:2485–97
Moster BP, Macciò AV, Somerville RS, Naab T, Cox TJ. 2011. *MNRAS* 415:3750–70
Moster BP, Naab T, White SDM. 2013. *MNRAS* 428:3121–38
Moster BP, Somerville RS, Maulbetsch C, et al. 2010. *Ap. J.* 710:903–23
Moustakas J, Coil AL, Aird J, et al. 2013. *Ap. J.* 767:50
Mulchaey JS. 2000. *Annu. Rev. Astron. Astrophys.* 38:289–335
Muratov AL, Kereš D, Faucher-Giguère CA, et al. 2015. *MNRAS* 454:2691–713
Murray N, Ménard B, Thompson TA. 2011. *Ap. J.* 735:66
Murray N, Quataert E, Thompson TA. 2005. *Ap. J.* 618:569–85
Murray N, Quataert E, Thompson TA. 2010. *Ap. J.* 709:191–209
Muzzin A, Marchesini D, Stefanon M, et al. 2013. *Ap. J.* 777:18
Naab T, Burkert A. 2003. *Ap. J.* 597:893–906
Naab T, Burkert A, Hernquist L. 1999. *Ap. J. Lett.* 523:L133–36
Naab T, Jesseit R, Burkert A. 2006a. *MNRAS* 372:839–52
Naab T, Johansson PH, Ostriker JP. 2009. *Ap. J. Lett.* 699:L178–82
Naab T, Johansson PH, Ostriker JP, Efstathiou G. 2007. *Ap. J.* 658:710–20
Naab T, Khochfar S, Burkert A. 2006b. *Ap. J. Lett.* 636:L81–84
Naab T, Oser L, Emsellem E, et al. 2014. *MNRAS* 444:3357–87
Naab T, Ostriker JP. 2009. *Ap. J.* 690:1452–62

Navarro JF, Benz W. 1991. *Ap. J.* 380:320–29
Navarro JF, Frenk CS, White SDM. 1995. *MNRAS* 275:56–66
Navarro JF, Steinmetz M. 1997. *Ap. J.* 478:13–28
Navarro JF, White SDM. 1993. *MNRAS* 265:271
Navarro JF, White SDM. 1994. *MNRAS* 267:401–12
Navarro-González J, Ricciardelli E, Quilis V, Vazdekis A. 2013. *MNRAS* 436:3507–24
Negroponte J, White SDM. 1983. *MNRAS* 205:1009–29
Nelson D, Genel S, Pillepich A, et al. 2016. *MNRAS* 460:2881–904
Nelson D, Genel S, Vogelsberger M, et al. 2015. *MNRAS* 448:59–74
Nelson D, Vogelsberger M, Genel S, et al. 2013. *MNRAS* 429:3353–70
Newman AB, Ellis RS, Bundy K, Treu T. 2012. *Ap. J.* 746:162
Newman SF, Genzel R, Förster-Schreiber NM, et al. 2012. *Ap. J.* 761:43
Nipoti C, Londrillo P, Ciotti L. 2003. *MNRAS* 342:501–12
Nipoti C, Treu T, Auger MW, Bolton AS. 2009. *Ap. J. Lett.* 706:L86–90
Noeske KG, Weiner BJ, Faber SM, et al. 2007. *Ap. J. Lett.* 660:L43–46
Norman CA, Ikeuchi S. 1989. *Ap. J.* 345:372–83
Novak GS, Ostriker JP, Ciotti L. 2011. *Ap. J.* 737:26
Okamoto T, Eke VR, Frenk CS, Jenkins A. 2005. *MNRAS* 363:1299–314
Okamoto T, Frenk CS, Jenkins A, Theuns T. 2010. *MNRAS* 406:208–22
Omma H, Binney J, Bryan G, Slyz A. 2004. *MNRAS* 348:1105–19
Oogi T, Habe A. 2013. *MNRAS* 428:641–57
Oppenheimer BD, Crain RA, Schaye J, et al. 2016. *MNRAS* 460:2157–79
Oppenheimer BD, Davé R. 2006. *MNRAS* 373:1265–92
Oppenheimer BD, Davé R. 2008. *MNRAS* 387:577–600
Oppenheimer BD, Davé R, Kereš D, et al. 2010. *MNRAS* 406:2325–38
Oppenheimer BD, Schaye J. 2013a. *MNRAS* 434:1043–62
Oppenheimer BD, Schaye J. 2013b. *MNRAS* 434:1063–78
Oser L, Naab T, Ostriker JP, Johansson PH. 2012. *Ap. J.* 744:63
Oser L, Ostriker JP, Naab T, Johansson PH, Burkert A. 2010. *Ap. J.* 725:2312
Ostriker EC, Shetty R. 2011. *Ap. J.* 731:41
Ostriker JP. 1980. *Comments Astrophys.* 8:177
Ostriker JP, Choi E, Ciotti L, Novak GS, Proga D. 2010. *Ap. J.* 722:642–52
Ostriker JP, Hausman MA. 1977. *Ap. J. Lett.* 217:L125–29
Ostriker JP, McKee CF. 1988. *Rev. Mod. Phys.* 60:1–68
Ostriker JP, Peebles PJE. 1973. *Ap. J.* 186:467–80
Ostriker JP, Thuan TX. 1975. *Ap. J.* 202:353–64
Pakmor R, Marinacci F, Springel V. 2014. *Ap. J. Lett.* 783:L20
Pakmor R, Pfrommer C, Simpson CM, Springel V. 2016. *Ap. J. Lett.* 824:L30
Pakmor R, Springel V. 2013. *MNRAS* 432:176–93
Patel SG, Fumagalli M, Franx M, et al. 2013a. *Ap. J.* 778:115
Patel SG, van Dokkum PG, Franx M, et al. 2013b. *Ap. J.* 766:15
Peters T, Naab T, Walch S, et al. 2016. *MNRAS* 466(3):3293–308
Peebles PJE. 1969. *Ap. J.* 155:393
Pelupessy FI, Di Matteo T, Ciardi B. 2007. *Ap. J.* 665:107–19
Pelupessy FI, Papadopoulos PP, van der Werf P. 2006. *Ap. J.* 645:1024–42
Pérez-González PG, Rieke GH, Villar V, et al. 2008. *Ap. J.* 675:234–61
Pettini M, Shapley AE, Steidel CC, et al. 2001. *Ap. J.* 554:981–1000
Pilkington K, Few CG, Gibson BK, et al. 2012. *Astron. Astrophys.* 540:A56
Piontek F, Steinmetz M. 2011. *MNRAS* 410:2625–42
Planck Collaboration, Ade PAR, Aghanim N, et al. 2014. *Astron. Astrophys.* 571:A16
Pontzen A, Governato F. 2012. *MNRAS* 421:3464–71
Poveda A, Ruiz J, Allen C. 1967. *Bol. Obs. Tonantzintla Tacubaya* 4:86–90
Price DJ, Federrath C. 2010. *MNRAS* 406:1659–74

Puchwein E, Springel V. 2013. *MNRAS* 428:2966–79
Puls J, Kudritzki RP, Herrero A, et al. 1996. *Astron. Astrophys.* 305:171–208
Qu Y, Di Matteo P, Lehnert M, van Driel W, Jog CJ. 2010. *Astron. Astrophys.* 515:A11
Qu Y, Helly JC, Bower RG, et al. 2017. *MNRAS* 464:1659–75
Quinn PJ, Hernquist L, Fullagar DP. 1993. *Ap. J.* 403:74–93
Rahmati A, Schaye J, Bower RG, et al. 2015. *MNRAS* 452:2034–56
Read JI, Hayfield T. 2012. *MNRAS* 422:3037–55
Rees MJ, Ostriker JP. 1977. *MNRAS* 179:541–59
Renaud F, Bournaud F, Duc PA. 2015. *MNRAS* 446:2038–54
Renaud F, Bournaud F, Emsellem E, et al. 2013. *MNRAS* 436:1836–51
Renzini A. 2006. *Annu. Rev. Astron. Astrophys.* 44:141–92
Renzini A, Andreon S. 2014. *MNRAS* 444:3581–91
Renzini A, Peng Y. 2015. *Ap. J. Lett.* 801:L29
Richings AJ, Schaye J. 2016. *MNRAS* 458:270–92
Richings AJ, Schaye J, Oppenheimer BD. 2014. *MNRAS* 442:2780–96
Rieder M, Teyssier R. 2016. *MNRAS* 457:1722–38
Rix HW, Bovy J. 2013. *Astron. Astrophys. Rev.* 21:61
Robertson B, Bullock JS, Cox TJ, et al. 2006a. *Ap. J.* 645:986–1000
Robertson B, Cox TJ, Hernquist L, et al. 2006b. *Ap. J.* 641:21–40
Robertson B, Hernquist L, Cox TJ, et al. 2006c. *Ap. J.* 641:90–102
Robertson B, Yoshida N, Springel V, Hernquist L. 2004. *Ap. J.* 606:32–45
Robertson BE, Kravtsov AV. 2008. *Ap. J.* 680:1083–111
Rodriguez-Gomez V, Pillepich A, Sales LV, et al. 2016. *MNRAS* 458:2371–90
Roos O, Juneau S, Bournaud F, Gabor JM. 2015. *Ap. J.* 800:19
Rosas-Guevara YM, Bower RG, Schaye J, et al. 2015. *MNRAS* 454:1038–57
Rosdahl J, Schaye J, Dubois Y, Kimm T, Teyssier R. 2017. *MNRAS* 466:11–33
Rosdahl J, Schaye J, Teyssier R, Agertz O. 2015. *MNRAS* 451:34–58
Roškar R, Teyssier R, Agertz O, Wetzstein M, Moore B. 2014. *MNRAS* 444:2837–53
Rothberg B, Joseph RD. 2004. *Astron. J.* 128:2098–143
Röttgers B, Naab T, Oser L. 2014. *MNRAS* 445:1065–83
Rubin KHR, Prochaska JX, Koo DC, et al. 2014. *Ap. J.* 794:156
Saintonge A, Kauffmann G, Kramer C, et al. 2011. *MNRAS* 415:32–60
Salem M, Bryan GL. 2014. *MNRAS* 437:3312–30
Salem M, Bryan GL, Corlies L. 2016. *MNRAS* 456:582–601
Sales LV, Marinacci F, Springel V, Petkova M. 2014. *MNRAS* 439:2990–3006
Sales LV, Navarro JF, Schaye J, et al. 2010. *MNRAS* 409:1541–56
Sánchez SF, Kennicutt RC, Gil de Paz A, et al. 2012. *Astron. Astrophys.* 538:A8
Sanders DB, Soifer BT, Elias JH, et al. 1988. *Ap. J.* 325:74–91
Sazonov SY, Ostriker JP, Ciotti L, Sunyaev RA. 2005. *MNRAS* 358:168–80
Sazonov SY, Ostriker JP, Sunyaev RA. 2004. *MNRAS* 347:144–56
Scalo J, Elmegreen BG. 2004. *Annu. Rev. Astron. Astrophys.* 42:275–316
Scannapieco C, Tissera PB, White SDM, Springel V. 2005. *MNRAS* 364:552–64
Scannapieco C, Tissera PB, White SDM, Springel V. 2006. *MNRAS* 371:1125–39
Scannapieco C, Wadepuhl M, Parry OH, et al. 2012. *MNRAS* 423:1726–49
Scannapieco C, White SDM, Springel V, Tissera PB. 2009. *MNRAS* 396:696–708
Scannapieco E, Brüggen M. 2008. *Ap. J.* 686:927–47
Scannapieco E, Brüggen M. 2015. *Ap. J.* 805:158
Schaller M, Dalla Vecchia C, Schaye J, et al. 2015. *MNRAS* 454:2277–91
Schawinski K, Treister E, Urry CM, et al. 2011. *Ap. J. Lett.* 727:L31
Schaye J, Crain RA, Bower RG, et al. 2015. *MNRAS* 446:521–54
Schaye J, Dalla Vecchia C. 2008. *MNRAS* 383:1210–22
Schaye J, Dalla Vecchia C, Booth CM, et al. 2010. *MNRAS* 402:1536–60
Schmidt M. 1959. *Ap. J.* 129:243

Sedov LI. 1959. *Similarity and Dimensional Methods in Mechanics.* New York: Academic
Serra P, Oosterloo T, Morganti R, et al. 2012. *MNRAS* 422:1835–62
Serra P, Oser L, Krajnović D, et al. 2014. *MNRAS* 444:3388–407
Shakura NI, Sunyaev RA. 1973. *Astron. Astrophys.* 24:337–55
Shankar F, Lapi A, Salucci P, De Zotti G, Danese L. 2006. *Ap. J.* 643:14–25
Shapley AE. 2011. *Annu. Rev. Astron. Astrophys.* 49:525–80
Sharma P, Roy A, Nath BB, Shchekinov Y. 2014. *MNRAS* 443:3463–76
Shen S, Mo HJ, White SDM, et al. 2003. *MNRAS* 343:978–94
Shlosman I, Frank J, Begelman MC. 1989. *Nature* 338:45–47
Sijacki D, Springel V, Di Matteo T, Hernquist L. 2007. *MNRAS* 380:877–900
Sijacki D, Vogelsberger M, Genel S, et al. 2015. *MNRAS* 452:575–96
Sijacki D, Vogelsberger M, Kereš D, Springel V, Hernquist L. 2012. *MNRAS* 424:2999–3027
Silk J. 1977. *Ap. J.* 211:638–48
Silk J, Rees MJ. 1998. *Astron. Astrophys.* 331:L1–4
Silva MDV, Napiwotzki R. 2011. *MNRAS* 411:2596–614
Simpson CM, Pakmor R, Marinacci F, et al. 2016. *Ap. J. Lett.* 827:L29
Skilling J. 1975. *MNRAS* 172:557–66
Slyz AD, Devriendt JEG, Bryan G, Silk J. 2005. *MNRAS* 356:737–52
Sofue Y, Rubin V. 2001. *Annu. Rev. Astron. Astrophys.* 39:137–74
Soltan A. 1982. *MNRAS* 200:115–22
Somerville RS, Davé R. 2015. *Annu. Rev. Astron. Astrophys.* 53:51–113
Somerville RS, Primack JR. 1999. *MNRAS* 310:1087–110
Sommer-Larsen J, Gelato S, Vedel H. 1999. *Ap. J.* 519:501–12
Sommer-Larsen J, Toft S. 2010. *Ap. J.* 721:1755–64
Song M, Finkelstein SL, Ashby MLN, Grazian A, Lu Y, et al. 2016. *Ap. J.* 825:5
Spergel DN, Bean R, Doré O, Nolta MR, Bennett CL, et al. 2007. *Ap. J. Suppl.* 170:377–408
Spitzer L Jr. 1978. *Physical Processes in the Interstellar Medium.* New York: John Wiley & Sons
Springel V. 2000. *MNRAS* 312:859–79
Springel V. 2005. *MNRAS* 364:1105–34
Springel V. 2010a. *Annu. Rev. Astron. Astrophys.* 48:391–430
Springel V. 2010b. *MNRAS* 401:791–851
Springel V, Di Matteo T, Hernquist L. 2005a. *Ap. J. Lett.* 620:L79–82
Springel V, Di Matteo T, Hernquist L. 2005b. *MNRAS* 361:776–94
Springel V, Hernquist L. 2003. *MNRAS* 339:289–311
Springel V, Hernquist L. 2005. *Ap. J. Lett.* 622:L9–12
Springel V, Wang J, Vogelsberger M, et al. 2008. *MNRAS* 391:1685–711
Springel V, White SDM, Jenkins A, et al. 2005c. *Nature* 435:629–36
Stadel J, Potter D, Moore B, et al. 2009. *MNRAS* 398:L21–25
Steidel CC, Erb DK, Shapley AE, et al. 2010. *Ap. J.* 717:289–322
Stinson G, Seth A, Katz N, et al. 2006. *MNRAS* 373:1074–90
Stinson GS, Bailin J, Couchman H, et al. 2010. *MNRAS* 408:812–26
Stinson GS, Brook C, Macciò AV, et al. 2013. *MNRAS* 428:129–40
Stone JM, Gardiner TA, Teuben P, et al. 2008. *Ap. J. Suppl.* 178:137–77
Strickland DK, Stevens IR. 2000. *MNRAS* 314:511–45
Strömgren B. 1939. *Ap. J.* 89:526–47
Strong AW, Moskalenko IV. 1998. *Ap. J.* 509:212–28
Strong AW, Moskalenko IV, Ptuskin VS. 2007. *Annu. Rev. Nucl. Part. Sci.* 57:285–327
Sun M, Voit GM, Donahue M, et al. 2009. *Ap. J.* 693:1142–72
Tabatabaei FS, Schinnerer E, Murphy EJ, et al. 2013. *Astron. Astrophys.* 552:A19
Tacconi LJ, Genzel R, Neri R, et al. 2010. *Nature* 463:781–84
Tacconi LJ, Neri R, Genzel R, et al. 2013. *Ap. J.* 768:74
Tammann GA, Loeffler W, Schroeder A. 1994. *Ap. J. Suppl.* 92:487–93
Taylor G. 1950. *Proc. R. Soc. Lond. Ser. A* 201:159–74

Teyssier R. 2002. *Astron. Astrophys.* 385:337–64
Teyssier R, Chapon D, Bournaud F. 2010. *Ap. J. Lett.* 720:L149–54
Teyssier R, Moore B, Martizzi D, Dubois Y, Mayer L. 2011. *MNRAS* 414:195–208
Teyssier R, Pontzen A, Dubois Y, Read JI. 2013. *MNRAS* 429:3068–78
Thacker RJ, Couchman HMP. 2000. *Ap. J.* 545:728–52
Thomas D, Maraston C, Bender R, Mendes de Oliveira C. 2005. *Ap. J.* 621:673–94
Toomre A, Toomre J. 1972. *Ap. J.* 178:623–66
Tornatore L, Borgani S, Dolag K, Matteucci F. 2007. *MNRAS* 382:1050–72
Treu T. 2010. *Annu. Rev. Astron. Astrophys.* 48:87–125
Trotta R, Jóhannesson G, Moskalenko IV, et al. 2011. *Ap. J.* 729:106
Truelove JK, McKee CF. 1999. *Ap. J. Suppl.* 120:299–326
Trujillo I, Conselice CJ, Bundy K, et al. 2007. *MNRAS* 382:109–20
Übler H, Naab T, Oser L, et al. 2014. *MNRAS* 443:2092–111
Uhlig M, Pfrommer C, Sharma M, et al. 2012. *MNRAS* 423:2374–96
Vale A, Ostriker JP. 2004. *MNRAS* 353:189–200
Vale A, Ostriker JP. 2006. *MNRAS* 371:1173–87
van den Bosch FC, Abel T, Croft RAC, Hernquist L, White SDM. 2002. *Ap. J.* 576:21–35
van der Kruit PC, Freeman KC. 2011. *Annu. Rev. Astron. Astrophys.* 49:301–71
van der Wel A, Franx M, van Dokkum PG, et al. 2014. *Ap. J.* 788:28
van Dokkum PG, Abraham R, Merritt A, et al. 2015. *Ap. J. Lett.* 798:L45
van Dokkum PG, Franx M, Kriek M, et al. 2008. *Ap. J. Lett.* 677:L5–8
van Dokkum PG, Whitaker KE, Brammer G, et al. 2010. *Ap. J.* 709:1018–41
Veilleux S, Cecil G, Bland-Hawthorn J. 2005. *Annu. Rev. Astron. Astrophys.* 43:769–826
Velazquez H, White SDM. 1999. *MNRAS* 304:254–70
VERITAS Collaboration, Acciari VA, Aliu E, et al. 2009. *Nature* 462:770–72
Vernaleo JC, Reynolds CS. 2006. *Ap. J.* 645:83–94
Vikhlinin A, Kravtsov A, Forman W, et al. 2006. *Ap. J.* 640:691–709
Villumsen JV. 1983. *MNRAS* 204:219–36
Vogelsberger M, Genel S, Sijacki D, et al. 2013. *MNRAS* 436:3031–67
Vogelsberger M, Genel S, Springel V, et al. 2014. *MNRAS* 444:1518–47
Völk HJ, Aharonian FA, Breitschwerdt D. 1996. *Space Sci. Rev.* 75:279–97
Wadepuhl M, Springel V. 2011. *MNRAS* 410:1975–92
Wadsley JW, Stadel J, Quinn T. 2004. *New Astron.* 9:137–58
Wadsley JW, Veeravalli G, Couchman HMP. 2008. *MNRAS* 387:427–38
Walch S, Girichidis P, Naab T, et al. 2015. *MNRAS* 454:238–68
Walch S, Naab T. 2015. *MNRAS* 451:2757–71
Walch SK, Whitworth AP, Bisbas T, Wünsch R, Hubber D. 2012. *MNRAS* 427:625–36
Wang L, Dutton AA, Stinson GS, et al. 2015. *MNRAS* 454:83–94
Watkins LL, Evans NW, An JH. 2010. *MNRAS* 406:264–78
Weil ML, Eke VR, Efstathiou G. 1998. *MNRAS* 300:773–89
Weinberger R, Springel V, Hernquist L, et al. 2017. *MNRAS* 465:3291–308
Wellons S, Torrey P, Ma CP, et al. 2016. *MNRAS* 456:1030–48
Werk JK, Prochaska JX, Tumlinson J, et al. 2014. *Ap. J.* 792:8
Wetzel AR, Hopkins PF, Kim Jh, et al. 2016. *Ap. J. Lett.* 827:L23
Whitaker KE, van Dokkum PG, Brammer G, Franx M. 2012. *Ap. J. Lett.* 754:L29
White SDM. 1978. *MNRAS* 184:185–203
White SDM. 1979a. *Ap. J. Lett.* 229:L9–13
White SDM. 1979b. *MNRAS* 189:831–52
White SDM, Rees MJ. 1978. *MNRAS* 183:341–58
Wiersma RPC, Schaye J, Smith BD. 2009. *MNRAS* 393:99–107
Williams RJ, Quadri RF, Franx M. 2011. *Ap. J. Lett.* 738:L25
Wise JH, Abel T, Turk MJ, Norman ML, Smith BD. 2012. *MNRAS* 427:311–26
Wong T, Blitz L. 2002. *Ap. J.* 569:157–83

Woods RM, Wadsley J, Couchman HMP, Stinson G, Shen S. 2014. *MNRAS* 442:732–40
Wu X, Gerhard O, Naab T, et al. 2014. *MNRAS* 438:2701–15
Wuyts S, Cox TJ, Hayward CC, et al. 2010. *Ap. J.* 722:1666–84
Wuyts S, Förster Schreiber NM, van der Wel A, et al. 2011. *Ap. J.* 742:96
Xue XX, Rix HW, Zhao G, et al. 2008. *Ap. J.* 684:1143–58
Yang HYK, Ruszkowski M, Ricker PM, Zweibel E, Lee D. 2012. *Ap. J.* 761:185
Yang X, Mo HJ, van den Bosch FC. 2003. *MNRAS* 339:1057–80
Yang X, Mo HJ, van den Bosch FC, et al. 2013. *Ap. J.* 770:115
Young LM, Bureau M, Davis TA, et al. 2011. *MNRAS* 414:940–67
Yuan F, Narayan R. 2014. *Annu. Rev. Astron. Astrophys.* 52:529–88
Zavala J, Frenk CS, Bower R, et al. 2016. *MNRAS* 460:4466–82
Zhukovska S, Dobbs C, Jenkins EB, Klessen RS. 2016. *Ap. J.* 831:147
Zweibel EG, Heiles C. 1997. *Nature* 385:131–36
Zwicky F. 1957. *Morphological Astronomy.* Berlin/Heidelburg: Springer-Verlag

Contents

Annual Review of Astronomy and Astrophysics

Volume 55, 2017

Indexes

Errata

An online log of corrections to *Annual Review of Astronomy and Astrophysics* articles may be found at http://www.annualreviews.org/errata/astro